International Journal of Computer Vision 50(3), 271–293, 2002

A Multiphase Level Set Framework for Image Segmentation Using the Mumford and Shah Model*

LUMINITA A. VESE AND TONY F. CHAN
Department of Mathematics, University of California, Los Angeles, California, USA

Received December 18, 2000; Revised July 2, 2002; Accepted July 10, 2002

Abstract. We propose a new multiphase level set framework for image segmentation using the Mumford and Shah model, for piecewise constant and piecewise smooth optimal approximations. The proposed method is also a generalization of an active contour model without edges based 2-phase segmentation, developed by the authors earlier in T. Chan and L. Vese (1999. In *Scale-Space'99*, M. Nilsen et al. (Eds.), LNCS, vol. 1682, pp. 141–151) and T. Chan and L. Vese (2001. IEEE-IP, 10(2):266–277). The multiphase level set formulation is new and of interest on its own: by construction, it automatically avoids the problems of vacuum and overlap; it needs only $\log n$ level set functions for n phases in the piecewise constant case; it can represent boundaries with complex topologies, including triple junctions; in the piecewise smooth case, only two level set functions formally suffice to represent any partition, based on The Four-Color Theorem. Finally, we validate the proposed models by numerical results for signal and image denoising and segmentation, implemented using the Osher and Sethian level set method.

Keywords: energy minimization, multi-phase motion, image segmentation, level sets, curvature, PDE's, denoising, edge detection, active contours

1. Introduction and Motivations, Related Relevant Work

The method introduced in this paper extends and generalizes the active contour model without edges based binary segmentation and level sets, previously proposed by the authors in Chan and Vese (1999, 2001). In that work, to obtain an active contour model for object detection, the basic idea was to look for a particular partition of a given image into two regions, one representing the objects to be detected, and the second one representing the background. The active contour was given by the boundary between these two regions. It turned out that the model was a particular case of the minimal partition problem of Mumford and Shah (1989) for segmentation of images. For the implementation of the active contour model from Chan and Vese (1999, 2001), the level set method of Osher and Sethian (1988) was successfully used, together with a particular numerical approximation, which allowed to automatically detect interior contours. The method was then easily extended to vector-valued images (Chan et al., 2000), and is robust with respect to noise.

In this paper, we generalize further this active contour model (based binary segmentation), to segment images with more than two regions, by proposing a new multiphase level set framework for the (Mumford and Shah, 1989) problem. We will show that, with a reduced number of level set functions, triple junctions and complex topologies can be represented. In addition, the phases used in the partition do not produce "vacuum" and "overlap." Finally, in the piecewise smooth case, based on The Four-Color Theorem, we show that only two level set functions formally should suffice to represent any partition.

The outline of the paper is as follows: in this Introduction, we give the necessary background on the

*The authors would like to dedicate this paper to Stanley Osher, on the occasion of his 60th birthday.

main two ingredients of the method: the Mumford and Shah model and variational level sets; then, we shortly describe the most related relevant work. In Section 2, we present the proposed model in the piecewise constant case in two dimensions, while in Section 3 we consider the piecewise smooth version of the model, in one and two dimensions. Finally, in Section 4 we present numerical results for signal and image denoising and segmentation, using the proposed models, and we end the paper by a short concluding section and an appendix, with the details of the numerical algorithms.

1.1. The Mumford and Shah Problem

Let $\Omega \subset \mathbb{R}^2$ be open and bounded. For the purpose of illustration, we consider for the moment the two-dimensional case, but any dimension could be considered. For instance, we will also treat the one-dimensional case in Section 3. Let C be a closed subset in Ω, made up of a finite set of smooth curves. The connected components of $\Omega \backslash C$ are denoted by Ω_i, such that $\Omega = \cup_i \Omega_i \cup C$. We also denote by $|C|$ the length of curves making up C. Let $u_0 : \Omega \to \mathbb{R}$ be a given bounded image-function.

The segmentation problem in computer vision, as formulated by Mumford and Shah (1989), can be defined as follows: given an observed image u_0, find a decomposition Ω_i of Ω and an optimal piecewise smooth approximation u of u_0, such that u varies smoothly within each Ω_i, and rapidly or discontinuously across the boundaries of Ω_i.

To solve this problem, Mumford and Shah (1989) proposed the following minimization problem:

$$\inf_{u,C} \left\{ F^{MS}(u, C) = \int_\Omega (u - u_0)^2 \, dx\, dy + \mu \int_{\Omega \backslash C} |\nabla u|^2 \, dx\, dy + \nu |C| \right\}, \quad (1)$$

where $\mu, \nu > 0$ are fixed parameters, to weight the different terms in the energy. For (u, C) a minimizer of the above energy, u is an "optimal" piecewise smooth approximation of the initial, possibly noisy, image u_0, and C has the role of approximating the edges of u_0; u will be smooth only outside C, i.e. on $\Omega \backslash C$. Theoretical results of existence and regularity of minimizers of (1) can be found for example in Mumford and Shah (1989), Morel and Solimini (1988, 1989, 1994), and De Giorgi et al. (1989).

A reduced case of the above model is obtained by restricting the segmented image u to piecewise constant functions, i.e. $u = \text{constant } c_i$ inside each connected component Ω_i. Then the problem is often called the "minimal partition problem," and in order to solve it, in Mumford and Shah (1989) it is proposed to minimize the following functional:

$$E^{MS}(u, C) = \sum_i \int_{\Omega_i} (u_0 - c_i)^2 \, dx\, dy + \nu |C|. \quad (2)$$

It is easy to see that, for a fixed C, the energy from (2) is minimized in the variables c_i by setting $c_i = mean(u_0)$ in Ω_i. Theoretical results for existence and regularity of minimizers of (2) can be found for example in Mumford and Shah (1989), Massari and Tamanini (1993), Tamanini (1996), Tamanini and Congedo (1996), and Leonardi and Tamanini (1998).

It is not easy to minimize in practice the functionals (1) and (2), because of the unknown set C of lower dimension, and also because the problems are not convex. After giving the necessary background on the level set method, we will review some alternative solutions to this problem, and other related relevant models for image segmentation, before presenting the proposed level set formulations.

1.2. The Level Set Method and Variational Level Sets

Osher and Sethian (1988) proposed an effective implicit representation for evolving curves and surfaces, which has found many applications, because it allows for automatic change of topology, such as merging and breaking, and the calculations are made on a fixed rectangular grid.

A given curve C (the boundary of an open set $\omega \in \Omega$, i.e. $C = \partial\omega$) is represented implicitly, as the zero level set of a scalar Lipschitz continuous function $\phi : \Omega \to \mathbb{R}$ (called level set function), such that (see Fig. 1):

$$\phi(x, y) > 0 \text{ in } \omega, \quad \phi(x, y) < 0 \text{ in } \Omega \backslash \omega,$$
$$\phi(x, y) = 0 \text{ on } \partial\omega.$$

A typical example of level set function is given by the signed distance function to the curve. Using this representation, geometrical quantities, properties and motions can be expressed. Indeed, using the Heaviside function $H(z)$, equal with 1 if $z \geq 0$ and with 0 if $z < 0$,

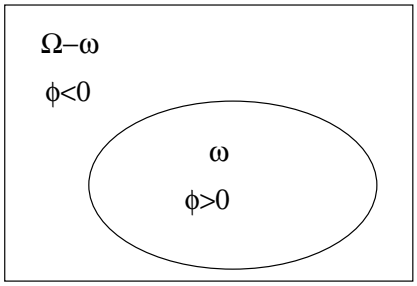

Figure 1. A curve, given by the zero level set of the function ϕ, is the boundary between the regions: $\{(x, y) : \phi(x, y) > 0\}$ and $\{(x, y) : \phi(x, y) < 0\}$.

the length of C and the area of ω can be expressed respectively by Evans and Gariepy (1992):

$$|C| = \int_\Omega |\nabla H(\phi)|, \quad |\omega| = \int_\Omega H(\phi)\, dx\, dy \qquad (3)$$

(we mention that the first integral is in the sense of measures).

Considering any $C^1(\mathbb{R})$ approximation and regularization H_ε of the Heaviside function as $\varepsilon \to 0$, and denoting by $\delta_\varepsilon = H'_\varepsilon$ (an approximation to the one-dimensional Dirac delta function δ_0), we can approximate the length functional by $L_\varepsilon(\phi) = \int_\Omega |\nabla H_\varepsilon(\phi)| dx dy = \int_\Omega \delta_\varepsilon(\phi)|\nabla\phi| dx dy$, and the area functional by $A_\varepsilon(\phi) = \int_\Omega H_\varepsilon(\phi) dx dy$.

Then we can formally write the associated Euler-Lagrange equations, obtained by minimizing the above functionals with respect to ϕ, and parameterizing the descent directions by an artificial time t, respectively (with associated initial conditions):

$$\frac{\partial\phi}{\partial t} = \delta_\varepsilon(\phi)\mathrm{div}\left(\frac{\nabla\phi}{|\nabla\phi|}\right), \quad \text{or} \quad \frac{\partial\phi}{\partial t} = \delta_\varepsilon(\phi).$$

A standard rescaling can be made, as in Zhao et al. (1996), by replacing $\delta_\varepsilon(\phi)$ by $|\nabla\phi|$, giving the following equations, already introduced in Osher and Sethian (1988) in the context of the level set theory:

$$\frac{\partial\phi}{\partial t} = |\nabla\phi|\mathrm{div}\left(\frac{\nabla\phi}{|\nabla\phi|}\right), \quad \text{or} \quad \frac{\partial\phi}{\partial t} = |\nabla\phi| \qquad (4)$$

(motion by mean curvature minimizing the length, and motion with constant speed minimizing the area). Here, $\frac{\nabla\phi}{|\nabla\phi|}$ represents the unit normal to a level curve of ϕ at every point, and $\mathrm{div}(\frac{\nabla\phi}{|\nabla\phi|})$ represents the curvature of the level curve.

For more recent and general expositions on the level set method and applications, we refer the reader to Sethian (1999), Osher and Fedkiw (2001, to appear). Theoretical results of existence, uniqueness, and regularity of the front for the equations from (4), in the sense of viscosity solutions, can be found in many papers, for instance in Barles (1994) for Hamilton-Jacobi equations, and in Evans and Spruck (1991), Chen et al. (1991), and Crandall et al. (1992), or more recently in Barles and Souganidis (1998), for generalized mean curvature flow equations and evolution of fronts.

1.3. Related Relevant Work for Image Segmentation

We briefly mention here some of the most related relevant works, and we discuss their connections or differences with our approach.

1.3.1. The Weak Formulation of the Mumford and Shah Problem and Approximations. A weak formulation of (1) has been proposed in De Giorgi and Ambrosio (1988), and studied in Dal Maso et al. (1992), where C is replaced by the set J_u of jumps of u, in order to prove the existence of minimizers (it is known that a global minimizer of (1), or of the weak formulation, is not unique in general). In Morel and Solimini (1988, 1989), the authors proposed a constructive existence result in the piecewise-constant case, and in Koepfler et al. (1994), a practical multi-scale algorithm based on regions growing and merging is proposed for this case. For a general exposition of the segmentation problem by variational methods, both in theory and practice, we refer the reader to Morel and Solimini (1994). We also refer to Ambrosio (1989) for theoretical results on functionals defined on the appropriate space for image segmentation: the $SBV(\Omega)$ space of special functions of bounded variation.

Two elliptic approximations by Γ-convergence to the weak formulation of the Mumford-Shah functional have been proposed in Ambrosio and Tortorelli (1990, 1992). They approximated a minimizer (u, J_u) of $F^{MS}(u, J_u)$, by two smooth functions (u_ρ, v_ρ), such that, as $\rho \to 0$, $u_\rho \to u$ and $v_\rho \to 1$ in the $L^2(\Omega)$-topology, and v_ρ is different from 1 only in a small neighborhood of J_u, which shrinks as $\rho \to 0$. The elliptic approximations lead to a coupled system of two equations in the unknowns u_ρ and v_ρ, to which standard PDE numerical methods can be applied.

Related approximations and numerical results can be found in March (1992), Chambolle (1992, 1995, 1999),

Bourdin and Chambolle (2000), and Bourdin (1999). Also, in Chambolle and Dal Maso (1999), the authors provide an approximation by Γ—*convergence* based on the finite element method, to the weak formulation.

Note that, most of the methods solving the weak formulation, do not explicitly compute the partition of the image and the set of curves C. In general (see for instance Ambrosio and Tortorelli (1990, 1992)), only an approximation to C is obtained, by a sequence of regions enclosing C, but converging in the limit to the empty set.

1.3.2. Active Contours Without Edges. We recall now the authors's active contour model without edges from Chan and Vese (1999, 2001), which is a particular case and the motivation of the proposed models from the present paper. Given the curve $C = \partial\omega$, with $\omega \subset \Omega$ an open subset, and two unknown constants c_1 and c_2, denoting $\Omega_1 = \omega$, $\Omega_2 = \Omega\backslash\omega$, we have proposed to minimize the following energy with respect to c_1, c_2 and C:

$$\begin{aligned} &F_2(c_1, c_2, C) \\ &\quad = \int_{\Omega_1=\omega} (u_0(x, y) - c_1)^2 \, dx\, dy \\ &\qquad + \int_{\Omega_2=\Omega\backslash\omega} (u_0(x, y) - c_2)^2 \, dx\, dy + \nu|C|, \end{aligned} \tag{5}$$

or in the level set formulation, with $C = \{(x, y) | \phi(x, y) = 0\}$:

$$\begin{aligned} F_2(c_1, c_2, \phi) = &\int_\Omega (u_0(x, y) - c_1)^2 H(\phi)\, dx\, dy \\ &+ \int_\Omega (u_0(x, y) - c_2)^2 (1 - H(\phi))\, dx\, dy \\ &+ \nu \int_\Omega |\nabla H(\phi)|. \end{aligned}$$

Considering H_ε and δ_ε any C^1 approximations and regularizations of the Heaviside function H and Delta function δ_0, as $\varepsilon \to 0$ and with $H'_\varepsilon = \delta_\varepsilon$, and minimizing the energy, we obtain: $\phi(0, x, y) = \phi_0(x, y)$:

$$c_1(\phi) = \frac{\int_\Omega u_0(x, y) H_\varepsilon(\phi(t, x, y))\, dx\, dy}{\int_\Omega H_\varepsilon(\phi(t, x, y))\, dx\, dy},$$

$$c_2(\phi) = \frac{\int_\Omega u_0(x, y)(1 - H_\varepsilon(\phi(t, x, y)))\, dx\, dy}{\int_\Omega (1 - H_\varepsilon(\phi(t, x, y)))\, dx\, dy},$$

$$\frac{\partial \phi}{\partial t} = \delta_\varepsilon(\phi)\left[\nu \mathrm{div}\left(\frac{\nabla \phi}{|\nabla \phi|}\right) - (u_0 - c_1)^2 + (u_0 - c_2)^2\right].$$

This model performs active contours, looking for a 2-phase segmentation of the image, given by $u(x, y) = c_1 H(\phi(x, y)) + c_2(1 - H(\phi(x, y)))$. The main advantages, by comparison with other active contour models, are: it automatically detects interior contours, the initial curve can be placed anywhere in the image, and it detects both contours with, or without gradient (called cognitive contours, following Kanizsa (1997)). Natural generalizations are presented in this paper, in Sections 2 and 3, for image segmentation, where more than two segments and non-constant regions can be represented, using a new multi-phase level set approach.

1.3.3. Inward and Outward Curve Evolution Using Level Set Method. A similar model with Chan and Vese (1999, 2001) was proposed in Amadieu et al. (1999). Again, this model is limited to object detection and two-phase segmentation, and it cannot segment images with more than two segments and with triple junctions, for instance. We will not give here the details of the model from Amadieu et al. (1999), being similar with that one from Chan and Vese (1999, 2001).

The previous two models already discussed above, Chan and Vese (1999, 2001) and Amadieu et al. (1999), cannot detect more than two segments and triple junctions. When working with level sets to represent triple junctions and more than two segments, the general idea is to use more then one level set function. Related relevant work is presented next, and this is the idea used in the proposed approach, but in a different way.

1.3.4. A Variational Level Set Approach to Multiphase Motion. The work from Zhao et al. (1996) is devoted to motion of junctions and boundaries of multiple phases, in a variational level set approach. Each phase Ω_i is represented via a level set function ϕ_i, such that $\Omega_i = \{(x, y) : \phi_i(x, y) > 0\}$. The total length of boundaries between phases is computed as $\frac{1}{2}\sum_i \int_\Omega |\nabla H(\phi_i)|$. In order to keep the phases disjoint (no overlap) and their union the domain Ω (no vacuum), the authors in Zhao et al. (1996) have added an additional term to the energy which is minimized, in the form $\lambda \int_\Omega (\sum_i H(\phi_i) - 1)^2 dx dy$. The Lagrange multiplier λ is updated at each time step, to keep the constraint $\sum_i H(\phi_i) = 1$ at all points satisfied. Motions of triple junctions are then obtained.

1.3.5. A Level Set Model for Image Classification. In Samson et al. (1999, 2000), the authors have applied the multi-phase level set representation from Zhao et al. (1996) to the reduced model of Mumford and Shah, for piecewise constant image segmentation. The problem is called classification, because the mean intensities c_i of classes are assumed to be known a-priori, and only the set of boundaries C is unknown.

1.3.6. A Statistical Approach to Snakes for Bimodal and Trimodal Imagery. In Yezzi et al. (1999), the authors are again using the idea of combining several level set functions, to represent more than two segments in an image. They are showing numerical results with binary flows (related with the models Chan and Vese (1999, 2001) and Amadieu et al. (1999)), but with additional choices for the segmentation criteria (instead of $\int_\Omega |u-u_0|^2 dxdy$, they propose other choices, with different statistical meanings). They also propose interesting ternary flows, where two evolving curves segment an image into three regions (two foreground regions and one background region).

1.3.7. Coupled Geodesic Active Regions for Image Segmentation: A Level Set Approach. In Paragios and Deriche (2000), the authors are using again multiple level set functions for image segmentation, in a probabilistic framework. As in Zhao et al. (1996) and Samson et al. (1999, 2000), each region is associated with one level set function. So, if N regions need to be segmented, then N level set functions are needed. Results of coupled curve evolution are obtained, to segment images with up to five different regions.

As we have seen, there are several choices for the representation of the different phases and their boundaries by level sets. As mentioned above, a first idea was proposed in Zhao et al. (1996), and then applied in Samson et al. (1999, 2000): a level set function is associated to each phase or each connected component Ω_i (this is also used in Paragios and Deriche (2000)). But then natural problems of vacuum and overlap appear, and these have been solved by adding additional constraints into the above mentioned models. An interesting idea, but different than ours, to remove the problems of vacuum and overlap, has been used in Merriman et al. (1994), but it is not clear how to incorporate this formulation into a variational framework. Their idea was that, at each step, after computing the characteristic functions χ_i, associated with each phase Ω_i, to re-define these characteristic functions by: $\chi_i(x, y) = \max\{\chi_j(x, y), 1 \leq j \leq \text{number of phases}\}$, to avoid the problems of vacuum and overlap. For another work on partitions, we also refer the reader to Ei et al. (1999). Finally, we would also like to refer to a projection method for motion of triple junctions by level sets (Smith et al., 2002).

In this paper, we propose a different multi-phase level set representation, and by construction, the distinct phases are disjoint (no overlap) and their union is the domain Ω (no vacuum); also, we need fewer level set functions to represent the same number of phases. Finally, we will see that triple junctions and other complex topologies can be detected and represented by the proposed multi-phase level set representation. Based on these characteristics, we think that the proposed approach is new and different than the existing related models. The applications of the proposed multi-phase level set formulation are devoted in this paper to image segmentation, via Mumford and Shah (1989).

Many other authors have studied the minimization of the Mumford-Shah functional and related problems for segmentation, both in theory and in practice, and it is impossible to mention all of them. However, we would like to mention Zhu et al. (1995), Zhu and Yuille (1996), Shah (1996, 1999), Shi and Malik (2000), and Sharon et al. (2000).

An interesting application of the level set method and energy minimization to segmentation of three-dimensional structures has been proposed in Lorigo et al. (1999), to extract complicated curve-like structures, such as blood vessels.

For general expositions on segmentation of images by variational methods, both in theory and algorithms, we refer the reader to Mumford et al. (1993) and Morel and Solimini (1994). Also, for recent expositions of geometric PDE's, variational problems and image processing (including snakes, active contours, curve evolution problems), we refer the reader to Sapiro (2001), Aubert and Kornprobst (2001), and Guichard and Morel (to appear).

To summarize, in this paper we propose: an extension and generalization of the active contour model without edges from Chan and Vese (1999, 2001), to the general Mumford and Shah model, in two cases: the piecewise constant case (2), and the piecewise smooth case (1). The proposed models can identify individual segments in images with multiple segments and junctions, as compared with the initial model (Chan and Vese, 1999, 2001), where the detected objects were belonging to the same segment. We also propose a new representation

for multiphase motion by level sets (requiring only $\log_2 n$ level set functions for n segments or phases in the piecewise constant case), allowing for triple junctions, for example, without vacuum or overlap between phases. In the piecewise smooth case, based on The Four-Color Theorem, we show that only two level set functions suffice for image segmentation. Finally, the proposed models inherit all the advantages of our active contour model without edges: detection of edges with or without gradient, detection of interior contours, automatic change of topology, robustness with respect to noise. The models can perform in parallel active contours, segmentation, denoising, object and edge detection.

2. Description of the Model in the Piecewise-Constant Case

In this section, we show how we can generalize the 2-phase piecewise constant active contour model without edges (Chan and Vese, 1999, 2001), to piecewise constant segmentation of images with more than two segments and junctions, using (2).

We note again that, using only one level set function, we can represent only two phases or segments in the image. Also, other geometrical features, such as triple junctions, cannot be represented using only one level set function. Our goal is to look for a new multiphase level set model with which we can represent more than two segments or phases, triple junctions and other complex topologies, in an efficient way. We will need only $\log_2 n$ level set functions to represent n phases or segments with complex topologies, such as triple junctions. In addition, our formulation automatically removes the problems of vacuum and overlap, because our partition is a disjoint decomposition and covering of the domain Ω by definition. This is explained next.

Let us consider $m = \log n$ level set functions $\phi_i : \Omega \to \mathbb{R}$. The union of the zero-level sets of ϕ_i will represent the edges in the segmented image. We also introduce the "vector level set function" $\Phi = (\phi_1, \ldots, \phi_m)$, and the "vector Heaviside function" $H(\Phi) = (H(\phi_1), \ldots, H(\phi_m))$ whose components are only 1 or 0. We can now define the segments or phases in the domain Ω, in the following way: two pixels (x_1, y_1) and (x_2, y_2) in Ω will belong to the same phase or class, if and only if $H(\Phi(x_1, y_1)) = H(\Phi(x_2, y_2))$. In other words, the classes or phases are given by the level sets of the function $H(\Phi)$, i.e. one class is formed by the set

$$\{(x, y) \mid H(\Phi(x, y)) = \text{constant vector} \in H(\Phi(\Omega))\}$$

(one phase or class contains those pixels (x, y) of Ω having the same value $H(\Phi(x, y))$).

There are up to $n = 2^m$ possibilities for the vector-values in the image of $H(\Phi)$. In this way, we can define up to $n = 2^m$ phases or classes in the domain of definition Ω. The classes defined in this way form a disjoint decomposition and covering of Ω. Therefore, each pixel $(x, y) \in \Omega$ will belong to one, and only one class, by definition, and there is no vacuum or overlap among the phases. This is an important advantage, comparing with the classical multiphase representation introduced in Zhao et al. (1996), and used in Samson et al. (1999, 2000). The set of curves C is represented by the union of the zero level sets of the functions ϕ_i.

We label the classes by I, with $1 \le I \le 2^m = n$. Now, let us introduce a constant vector of averages $c = (c_1, \ldots, c_n)$, where $c_I = mean(u_0)$ in the class I, and the characteristic function χ_I for each class I. Then the reduced Mumford-Shah energy (2) can be written as:

$$F_n^{MS}(c, \Phi) = \sum_{1 \le I \le n = 2^m} \int_\Omega (u_0(x, y) - c_I)^2 \chi_I \, dx\, dy + \nu \frac{1}{2} \sum_{1 \le I \le n = 2^m} \int_\Omega |\nabla \chi_I|. \tag{6}$$

In order to simplify the model, we will replace the length term by $\sum_i \int_\Omega |\nabla H(\phi_i)|$ (i.e. the sum of the length of the zero-level sets of ϕ_i). Thus, in some cases, some parts of the curves will count more than once in the total length term, or in other words, some edges will have a different weight in the total length term. We will see that with this slight modification and simplification, we still obtain very satisfactory results (it may have only a very small effect in most of the cases, because the fitting term is dominant).

Therefore, the energy that we will minimize is given by:

$$F_n(c, \Phi) = \sum_{1 \le I \le n = 2^m} \int_\Omega (u_0 - c_I)^2 \chi_I \, dx\, dy + \sum_{1 \le i \le m} \nu \int_\Omega |\nabla H(\phi_i)|. \tag{7}$$

Clearly, for $n = 2$ (and therefore $m = 1$), we obtain the 2-phase energy (5) considered in our active contour

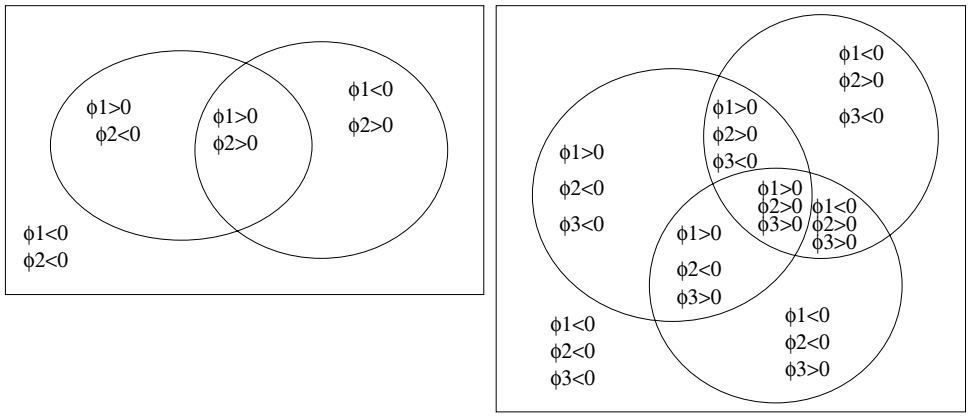

Figure 2. Left: 2 curves $\{\phi_1 = 0\} \cup \{\phi_2 = 0\}$ partition the domain into 4 regions: $\{\phi_1 > 0, \phi_2 > 0\}$, $\{\phi_1 > 0, \phi_2 < 0\}$, $\{\phi_1 < 0, \phi_2 > 0\}$, $\{\phi_1 < 0, \phi_2 < 0\}$. Right: 3 curves $\{\phi_1 = 0\} \cup \{\phi_2 = 0\} \cup \{\phi_3 = 0\}$ partition the domain into 8 regions: $\{\phi_1 > 0, \phi_2 > 0, \phi_3 > 0\}$, $\{\phi_1 > 0, \phi_2 > 0, \phi_3 < 0\}$, $\{\phi_1 > 0, \phi_2 < 0, \phi_3 > 0\}$, $\{\phi_1 > 0, \phi_2 < 0, \phi_3 < 0\}$, $\{\phi_1 < 0, \phi_2 > 0, \phi_3 > 0\}$, $\{\phi_1 < 0, \phi_2 > 0, \phi_3 < 0\}$, $\{\phi_1 < 0, \phi_2 < 0, \phi_3 > 0\}$, $\{\phi_1 < 0, \phi_2 < 0, \phi_3 < 0\}$.

model without edges. For the purpose of illustration, let us write the above energy for $n = 4$ phases or classes (and therefore using $m = 2$ level set functions; see Fig. 2 left):

$$\begin{aligned} F_4(c, \Phi) &= \int_\Omega (u_0 - c_{11})^2 H(\phi_1) H(\phi_2)\, dx\, dy \\ &\quad + \int_\Omega (u_0 - c_{10})^2 H(\phi_1)(1 - H(\phi_2))\, dx\, dy \\ &\quad + \int_\Omega (u_0 - c_{01})^2 (1 - H(\phi_1)) H(\phi_2)\, dx\, dy \\ &\quad + \int_\Omega (u_0 - c_{00})^2 (1 - H(\phi_1))(1 - H(\phi_2))\, dx\, dy \\ &\quad + \nu \int_\Omega |\nabla H(\phi_1)| + \nu \int_\Omega |\nabla H(\phi_2)|, \end{aligned} \tag{8}$$

where $c = (c_{11}, c_{10}, c_{01}, c_{00})$ is a constant vector, and $\Phi = (\phi_1, \phi_2)$.

With these notations, we can express the image-function u as:

$$\begin{aligned} u &= c_{11} H(\phi_1) H(\phi_2) + c_{10} H(\phi_1)(1 - H(\phi_2)) \\ &\quad + c_{01}(1 - H(\phi_1)) H(\phi_2) \\ &\quad + c_{00}(1 - H(\phi_1))(1 - H(\phi_2)). \end{aligned}$$

The Euler-Lagrange equations obtained by minimizing (8) with respect to c and Φ, embedded in a dynamical scheme, are: given $\phi_1(0, x, y) = \phi_{1,0}(x, y)$, $\phi_2(0, x, y) = \phi_{2,0}(x, y)$,

$$\begin{aligned} c_{11}(\Phi) = \mathit{mean}(u_0) \text{ in } \{(x, y) : \phi_1(t, x, y) > 0, \\ \phi_2(t, x, y) > 0\} \end{aligned}$$

$$\begin{aligned} c_{10}(\Phi) = \mathit{mean}(u_0) \text{ in } \{(x, y) : \phi_1(t, x, y) > 0, \\ \phi_2(t, x, y) < 0\} \end{aligned}$$

$$\begin{aligned} c_{01}(\Phi) = \mathit{mean}(u_0) \text{ in } \{(x, y) : \phi_1(t, x, y) < 0, \\ \phi_2(t, x, y) > 0\} \end{aligned}$$

$$\begin{aligned} c_{00}(\Phi) = \mathit{mean}(u_0) \text{ in } \{(x, y) : \phi_1(t, x, y) < 0, \\ \phi_2(t, x, y) < 0\}, \end{aligned}$$

$$\begin{aligned} \frac{\partial \phi_1}{\partial t} &= \delta_\varepsilon(\phi_1) \Bigg\{ \nu \mathrm{div}\left(\frac{\nabla \phi_1}{|\nabla \phi_1|} \right) \\ &\quad - [((u_0 - c_{11})^2 - (u_0 - c_{01})^2) H(\phi_2) \\ &\quad + ((u_0 - c_{10})^2 - (u_0 - c_{00})^2)(1 - H(\phi_2))] \Bigg\}, \\ \frac{\partial \phi_2}{\partial t} &= \delta_\varepsilon(\phi_2) \Bigg\{ \nu \mathrm{div}\left(\frac{\nabla \phi_2}{|\nabla \phi_2|} \right) \\ &\quad - [((u_0 - c_{11})^2 - (u_0 - c_{10})^2) H(\phi_1) \\ &\quad + ((u_0 - c_{01})^2 - (u_0 - c_{00})^2)(1 - H(\phi_1))] \Bigg\}. \end{aligned}$$

We note that the equations in $\Phi = (\phi_1, \phi_2)$ are governed by both mean curvature and jump of the data energy terms across the boundary.

We show in Fig. 2 right, the partition of the domain Ω into eight regions, using three level set functions.

It is easy to extend the proposed model to vector-valued functions, such as color images, following for instance (Chan et al. 2000). In this case, $u_0 = (u_{0,1}, \ldots, u_{0,N})$ is the initial data, with N channels ($N = 3$ for color RGB images), and for each channel $i = 1, \ldots, N$, we have the constants

$c_I = (c_{I,1}, \ldots, c_{I,N})$. In this case, the model for multichannel segmentation will be:

$$F_n(c_I, \Phi) = \sum_{1 \le I \le n = 2^m} \sum_{i=1}^{N} \int_\Omega |u_{0,i} - c_{I,i}|^2 \chi_I \, dx \, dy + \sum_{1 \le i \le m} \nu \int_\Omega |\nabla H(\phi_i)|.$$

Note that, even if we work with vector-valued images, the level set functions are the same for all channels (i.e. we do not need additional level set functions for each channel). The associated Euler-Lagrange equations can easily be deduced.

3. Description of the Model in the Piecewise-Smooth Case

In this section, we propose a multi-phase level set formulation and algorithm for the general problem of Mumford and Shah (1989) in image processing (1), to compute piecewise smooth optimal approximations of a given image. We consider the cases:

(1) In one dimension: for signal segmentation and denoising, we show that, using only one level set function, we can represent any signal with any number of segments in the partition.
(2) In two dimensions:
   (i) we generalize the 2-phase piecewise-constant model from Chan and Vese (1999, 2001), to piecewise-smooth optimal approximations using only one level set function: different regions of distinct intensities can be represented and detected with the correct intensities.
   (ii) following the idea of the multi-phase level set partition from the previous section, we show that, in the piecewise-smooth case, using only two level set functions, producing up to four phases, any general case can be considered and represented by the proposed formulation. Our main idea is based on The Four-Color Theorem.

3.1. The One-Dimensional Case: Signal Denoising and Segmentation

In many applications, we deal with a source signal u on $\Omega = (a, b)$. The problem of reconstructing u from a disturbed input u_0 deriving from a distorted transmission, can be modeled as finding the minimum

$$\min_{u,C} \left\{ \mu \int_{(a,b)\setminus C} |u'|^2 dx + \int_a^b |u - u_0|^2 dx + \nu \#(C) \right\}, \tag{9}$$

where C denotes the set of discontinuity points of u, and $\#(C)$ denotes the cardinal of C (the counting measure).

We let $C = \{x \in (a, b) \,|\, \phi(x) = 0\}$, with ϕ being a one dimensional level set function, and we introduce two functions u^+ and u^-, such that $u(x) = u^+(x)H(\phi(x)) + u^-(x)(1 - H(\phi(x))$. These two functions replace the two unknown constants used in Chan and Vese (1999, 2001), and are such that $u^+ \in C^1(\{\phi \ge 0\})$, and $u^- \in C^1(\{\phi \le 0\})$. Then the energy (9) can be written in the level set formulation as:

$$\begin{aligned} \min_{u^+,u^-,\phi} \Bigg\{ & \mu \int_a^b |(u^+)'|^2 H(\phi)\, dx \\ & + \mu \int_a^b |(u^-)'|^2 (1 - H(\phi))\, dx \\ & + \int_a^b |u^+ - u_0|^2 H(\phi)\, dx \\ & + \int_a^b |u^- - u_0|^2 (1 - H(\phi))\, dx \\ & + \nu \int_a^b |H(\phi)'|. \Bigg\} \end{aligned}$$

Minimizing this energy with respect to u^+, u^-, and ϕ, we obtain the associated Euler-Lagrange equations, embedded in a dynamical scheme:

$$\begin{aligned} u^+ &= u_0 + \mu (u^+)'' \text{ in } \{x : \phi(t, x) > 0\}, \\ (u^+)' &= 0 \text{ on } \{x : \phi(t, x) = 0\}, \\ u^- &= u_0 + \mu (u^-)'' \text{ in } \{x : \phi(t, x) < 0\}, \\ (u^-)' &= 0 \text{ on } \{x : \phi(t, x) = 0\}, \\ \frac{\partial \phi}{\partial t} &= \delta_\varepsilon(\phi) \Bigg[\nu \left(\frac{\phi'}{|\phi'|} \right)' - |u^+ - u_0|^2 + |u^- - u_0|^2 \\ &\qquad - \mu |(u^+)'|^2 + \mu |(u^-)'|^2 \Bigg]. \end{aligned}$$

Note that, in one dimension for signal segmentation, only one level set function suffices to represent a piecewise smooth function u, together with its set of jumps.

3.2. The Two-Dimensional Case: Two-Phase Model

We consider the corresponding two-dimensional case, under the assumption that the edges (denoted by C) in

the image can be represented by one level set function ϕ, i.e. $C = \{(x, y) \,|\, \phi(x, y) = 0\}$. The most general case, allowing for any type of edges, including triple junctions, will also be considered.

As in the 1-dimensional case, the link between the unknowns u and ϕ can be expressed by introducing two functions u^+ and u^-, such that

$$u(x, y) = \begin{cases} u^+(x, y) & \text{if } \phi(x, y) \geq 0, \\ u^-(x, y) & \text{if } \phi(x, y) < 0. \end{cases}$$

We assume that u^+ and u^- are C^1 functions on $\phi \geq 0$ and on $\phi \leq 0$ respectively (and therefore with continuous derivatives up to all boundary points, i.e. up to the boundary $\{\phi = 0\}$). We illustrate our formulation in Fig. 3 (left).

Then we obtain the following minimization problem from (1):

$$\begin{aligned} \inf_{u^+, u^-, \phi} \Bigg\{ F(u^+, u^-, \phi) &= \int_\Omega |u^+ - u_0|^2 H(\phi)\, dx\, dy \\ &+ \int_\Omega |u^- - u_0|^2 (1 - H(\phi))\, dx\, dy \\ &+ \mu \int_\Omega |\nabla u^+|^2 H(\phi))\, dx\, dy \\ &+ \mu \int_\Omega |\nabla u^-|^2 (1 - H(\phi))\, dx\, dy \\ &+ \nu \int_\Omega |\nabla H(\phi)|. \Bigg\} \end{aligned}$$

Minimizing $F(u^+, u^-, \phi)$ with respect to u^+, u^-, and ϕ, we obtain the following Euler-Lagrange equations (embedded in a dynamical scheme for ϕ):

$$\begin{aligned} u^+ - u_0 &= \mu \triangle u^+ \text{ in } \{(x, y) : \phi(t, x, y) > 0\}, \\ \frac{\partial u^+}{\partial \vec{n}} &= 0 \text{ on } \{(x, y) : \phi(t, x, y) = 0\} \cup \partial\Omega, \end{aligned} \quad (10)$$

$$\begin{aligned} u^- - u_0 &= \mu \triangle u^- \text{ in } \{(x, y) : \phi(t, x, y) < 0\}, \\ \frac{\partial u^-}{\partial \vec{n}} &= 0 \text{ on } \{(x, y) : \phi(t, x, y) = 0\} \cup \partial\Omega, \end{aligned} \quad (11)$$

$$\begin{aligned} \frac{\partial \phi}{\partial t} = \delta_\varepsilon(\phi) \Bigg[\nu \nabla \left(\frac{\nabla \phi}{|\nabla \phi|} \right) - |u^+ - u_0|^2 - \mu |\nabla u^+|^2 \\ + |u^- - u_0|^2 + \mu |\nabla u^-|^2 \Bigg], \end{aligned} \quad (12)$$

where $\partial / \partial \vec{n}$ denotes the partial derivative in the normal direction $\vec{n}$ at the corresponding boundary. We also associate the boundary condition $\frac{\partial \phi}{\partial \vec{n}} = 0$ on $\partial\Omega$ to Eq. (12).

The equations for u^+ and u^- will have a smoothing and denoising effect on the image u_0, but only inside homogeneous regions, and not across edges.

We would like to mention that ideas very similar with those from the above case, have been also developed by Tsai et al. (2001), independently and contemporaneously. Also, after this work had been completed, the authors noticed that L. Cohen and collaborators have previously used a level set method for a variant of the Mumford and Shah model, related with the one described in this subsection. The authors used this to detect the boundary of a lake (see Cohen et al., 1993; Cohen, 1997).

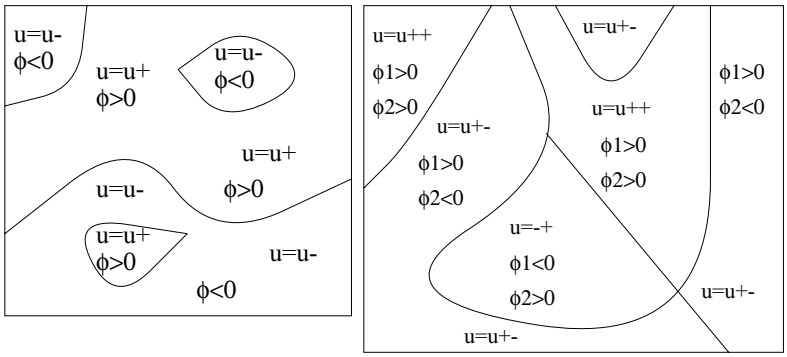

Figure 3. Left: example of partition of the image u in regions with boundaries represented via a single level set function $\{\phi = 0\}$, and with smooth value-functions u^+, u^- on each side of the curve. Right: example of partition of the image u in regions with boundaries represented via two level set functions $\{\phi_1 = 0\} \cup \{\phi_2 = 0\}$, and with smooth value-functions u^{++}, u^{+-}, u^{-+} and u^{--}, on all sides of the curves.

3.3. The Two-Dimensional Case: Four-Phase Model

In the previous two cases, we have shown how we can minimize the general Mumford-Shah functional for segmentation in the case where the set of contours C can be represented by a single level set function, i.e. $C = \{\phi = 0\}$ and ϕ has opposite signs on each side of C. By this method, we can already detect several objects of distinct gray-levels, but we have a constraint on the type of edges. There are cases where the boundaries of regions forming a partition of the image could not be represented in this way (i.e. using a single level set function). Again, the natural idea is to use more than one level set function, as in Section 2.

We show that in the general case, the problem can be solved using only two level set functions, and we do not have to know a-priori how many gray-levels the image has (or how many segments). The idea is based on The Four-Color Theorem and is as follows.

Based on this observation, we can "color" all the regions in a partition using only four "colors," such that any two adjacent regions have different "colors." Therefore, using two level set functions, we can identify the four "colors" by the following (disjoint) sets: $\{\phi_1 > 0, \phi_2 > 0\}$, $\{\phi_1 > 0, \phi_2 < 0\}$, $\{\phi_1 < 0, \phi_2 > 0\}$, $\{\phi_1 < 0, \phi_2 < 0\}$. The boundaries of the regions forming the partition will be given by $\{\phi_1 = 0\} \cup \{\phi_2 = 0\}$, and this will be the set of curves C. Again, in our particular multiphase formulation of the problem, we do not have the problems of "overlapping" or "vacuum," (i.e. the phases are disjoint, and their union is the entire domain Ω).

As in the previous case, the link between the function u and the four regions can be made by introducing four functions $u^{++}, u^{+-}, u^{-+}, u^{--}$, which are in fact the restrictions of u to each of the four phases, as follows:

$$u(x, y) = \begin{cases} u^{++}(x, y), & \text{if } \phi_1(x, y) > 0 \text{ and } \phi_2(x, y) > 0, \\ u^{+-}(x, y), & \text{if } \phi_1(x, y) > 0 \text{ and } \phi_2(x, y) < 0, \\ u^{-+}(x, y), & \text{if } \phi_1(x, y) < 0 \text{ and } \phi_2(x, y) > 0, \\ u^{--}(x, y), & \text{if } \phi_1(x, y) < 0 \text{ and } \phi_2(x, y) < 0. \end{cases}$$

These notations are illustrated in Fig. 3 (right).

Again, using the Heaviside function, the relation between u, the four functions u^{++}, u^{+-}, u^{-+}, u^{--}, and the level set functions ϕ_1 and ϕ_2 can be expressed by:

$$\begin{aligned} u = {} & u^{++}H(\phi_1)H(\phi_2) + u^{+-}H(\phi_1)(1 - H(\phi_2)) \\ & + u^{-+}(1 - H(\phi_1))H(\phi_2) \\ & + u^{--}(1 - H(\phi_1))(1 - H(\phi_2)). \end{aligned}$$

Using the notation $\Phi = (\phi_1, \phi_2)$, we introduce an energy in level set formulation, based on the Mumford-Shah functional (1):

$$\begin{aligned} & F(u, \Phi) \\ & = \int_\Omega |u^{++} - u_0|^2 H(\phi_1)H(\phi_2)\,dx\,dy \\ & \quad + \mu \int_\Omega |\nabla u^{++}|^2 H(\phi_1)H(\phi_2)\,dx\,dy \\ & \quad + \int_\Omega |u^{+-} - u_0|^2 H(\phi_1)(1 - H(\phi_2))\,dx\,dy \\ & \quad + \mu \int_\Omega |\nabla u^{+-}|^2 H(\phi_1)(1 - H(\phi_2))\,dx\,dy \\ & \quad + \int_\Omega |u^{-+} - u_0|^2 (1 - H(\phi_1))H(\phi_2)\,dx\,dy \\ & \quad + \mu \int_\Omega |\nabla u^{-+}|^2 (1 - H(\phi_1))H(\phi_2)\,dx\,dy \\ & \quad + \int_\Omega |u^{--} - u_0|^2 (1 - H(\phi_1))(1 - H(\phi_2))\,dx\,dy \\ & \quad + \mu \int_\Omega |\nabla u^{--}|^2 (1 - H(\phi_1))(1 - H(\phi_2))\,dx\,dy \\ & \quad + \nu \int_\Omega |\nabla H(\phi_1)| + \nu \int_\Omega |\nabla H(\phi_2)|. \end{aligned}$$

As in Section 2, we note that the expression $\int_\Omega |\nabla H(\phi_1)| + \int_\Omega |\nabla H(\phi_2)|$ is not exactly the length term of C, it is just an approximation and simplification. In practice, we have obtained satisfactory results using the above formula, and the associated Euler-Lagrange equations are simplified.

We obtain the associated Euler-Lagrange equations as in the previous cases, embedded in a dynamic scheme, assuming $(t, x, y) \mapsto \phi_i(t, x, y)$: minimizing the energy with respect to the functions u^{++}, u^{+-}, u^{-+}, u^{--}, we have, for each fixed t:

$$\begin{aligned} & u^{++} - u_0 = \mu \triangle u^{++} \text{ in } \{\phi_1 > 0, \phi_2 > 0\}, \\ & \quad \frac{\partial u^{++}}{\partial \vec{n}} = 0 \text{ on } \{\phi_1 = 0, \phi_2 \geq 0\}, \{\phi_1 \geq 0, \phi_2 = 0\}; \\ & u^{+-} - u_0 = \mu \triangle u^{+-} \text{ in } \{\phi_1 > 0, \phi_2 < 0\}, \\ & \quad \frac{\partial u^{+-}}{\partial \vec{n}} = 0 \text{ on } \{\phi_1 = 0, \phi_2 \leq 0\}, \{\phi_1 \geq 0, \phi_2 = 0\}; \end{aligned}$$

$$
\begin{aligned}
&u^{-+} - u_0 = \mu \triangle u^{-+} \text{ in } \{\phi_1 < 0, \phi_2 > 0\},\\
&\quad \frac{\partial u^{-+}}{\partial \vec{n}} = 0 \text{ on } \{\phi_1 = 0, \phi_2 \geq 0\}, \{\phi_1 \leq 0, \phi_2 = 0\};\\
&u^{--} - u_0 = \mu \triangle u^{--} \text{ in } \{\phi_1 < 0, \phi_2 < 0\},\\
&\quad \frac{\partial u^{--}}{\partial \vec{n}} = 0 \text{ on } \{\phi_1 = 0, \phi_2 \leq 0\}, \{\phi_1 \leq 0, \phi_2 = 0\}.
\end{aligned}
$$

The Euler-Lagrange equations evolving ϕ_1 and ϕ_2, embedded in a dynamic scheme, formally are:

$$
\begin{aligned}
\frac{\partial \phi_1}{\partial t} = \delta_\varepsilon(\phi_1)\Bigg[& \nu \nabla\left(\frac{\nabla \phi_1}{|\nabla \phi_1|}\right) - |u^{++} - u_0|^2 H(\phi_2)\\
& - \mu |\nabla u^{++}|^2 H(\phi_2) - |u^{+-} - u_0|^2 (1 - H(\phi_2))\\
& - \mu |\nabla u^{+-}|^2 (1 - H(\phi_2)) + |u^{-+} - u_0|^2 H(\phi_2)\\
& + \mu |\nabla u^{-+}|^2 H(\phi_2) + |u^{--} - u_0|^2 (1 - H(\phi_2))\\
& + \mu |\nabla u^{--}|^2 (1 - H(\phi_2))\Bigg] = 0,
\end{aligned}
$$

$$
\begin{aligned}
\frac{\partial \phi_2}{\partial t} = \delta_\varepsilon(\phi_2)\Bigg[& \nu \nabla\left(\frac{\nabla \phi_2}{|\nabla \phi_2|}\right) - |u^{++} - u_0|^2 H(\phi_1)\\
& - \mu |\nabla u^{++}|^2 H(\phi_1) + |u^{+-} - u_0|^2 H(\phi_1)\\
& + \mu |\nabla u^{+-}|^2 H(\phi_1) - |u^{-+} - u_0|^2 (1 - H(\phi_1))\\
& - \mu |\nabla u^{-+}|^2 (1 - H(\phi_1)) + |u^{--} - u_0|^2\\
& \times (1 - H(\phi_1)) + \mu |\nabla u^{--}|^2 (1 - H(\phi_1))\Bigg].
\end{aligned}
$$

We have mentioned in the introduction existence results for the Mumford-Shah minimization problem. The global minimizer is not unique in general. We can also show, by standard techniques of the calculus of variations on the spaces $BV(\Omega)$ and $SBV(\Omega)$ (functions of bounded variation and special functions of bounded variation respectively), and a compactness result due to Ambrosio (1989), that the proposed minimization problems from this paper, in the level set formulation, have a minimizer. Finally, because there is no uniqueness among minimizers, and because the problems are non-convex, the numerical results may depend on the initial choice of the curves, and we may compute a local minimum only. We think that, using the seed initialization (see Section 4), the algorithms have the tendency of computing a global minimum.

4. Numerical Results

We fix the space steps $h = \triangle x = \triangle y = 1$, the time step $\triangle t = 0.1$, and $\varepsilon = h$.

4.1. Numerical Results in the Piecewise-Constant Case (2D)

We show now numerical results using the models from Section 2, and in particular using the four-phase (with two level set functions) and the eight-phase (with three level set functions) models. The only varying parameter is ν, the coefficient of the length term. We give the cpu time in seconds for our calculations, performed on a 140 MHz Sun Ultra 1 with 256 MB of RAM. In our numerical algorithm, we first initialize the level set functions by ϕ_i^0, then we compute the averages c_I, and we solve one step of the PDE's in ϕ_i. Then we iterate these last two steps.

We show in particular that triple junctions can be represented and detected using only two level set functions, that interior contours are automatically detected and also that the model is robust in the presence of noise and complex topologies.

We begin with a noisy synthetic image with four regions (Figs. 4, 5 and 6), and we consider several different initial conditions. For the initial conditions (a), (b), (c) we use the four-phase piecewise constant model, while for (d) we use the eight-phase piecewise constant model. The energy decrease is shown in Fig. 4 bottom for the initial conditions (a)–(d). The image contains three objects of distinct intensities, all correctly detected and segmented for initial conditions (a), (c), (d). This is an improvement of the authors previous 2-phase active contour model (Chan and Vese, 1999, 2001), with which all three objects would have the same intensity in the segmented image, belonging to the same segment or phase.

Because the energy which is minimized is not convex, and also that there is no uniqueness for the minimizers, the algorithm may not converge to a global minimizer for a given initial condition. It is then natural to consider different initial conditions for the same image with the same parameters, and to compare the steady-state solutions from our numerical algorithm. For (c), we seed with small initial curves. Only using the initial conditions (a), (c), (d) do we compute a global minimizer for this image. For (b), the algorithm is trapped in a local minimum. In general, for real images with more complicated features, we think that initial conditions of the types (c), (d) should be used, which have the tendency to converge to a global minimizer. This type of initial condition is also related to the region growing algorithm (Koepfler et al., 1994). We also note that using the initial condition (c), the

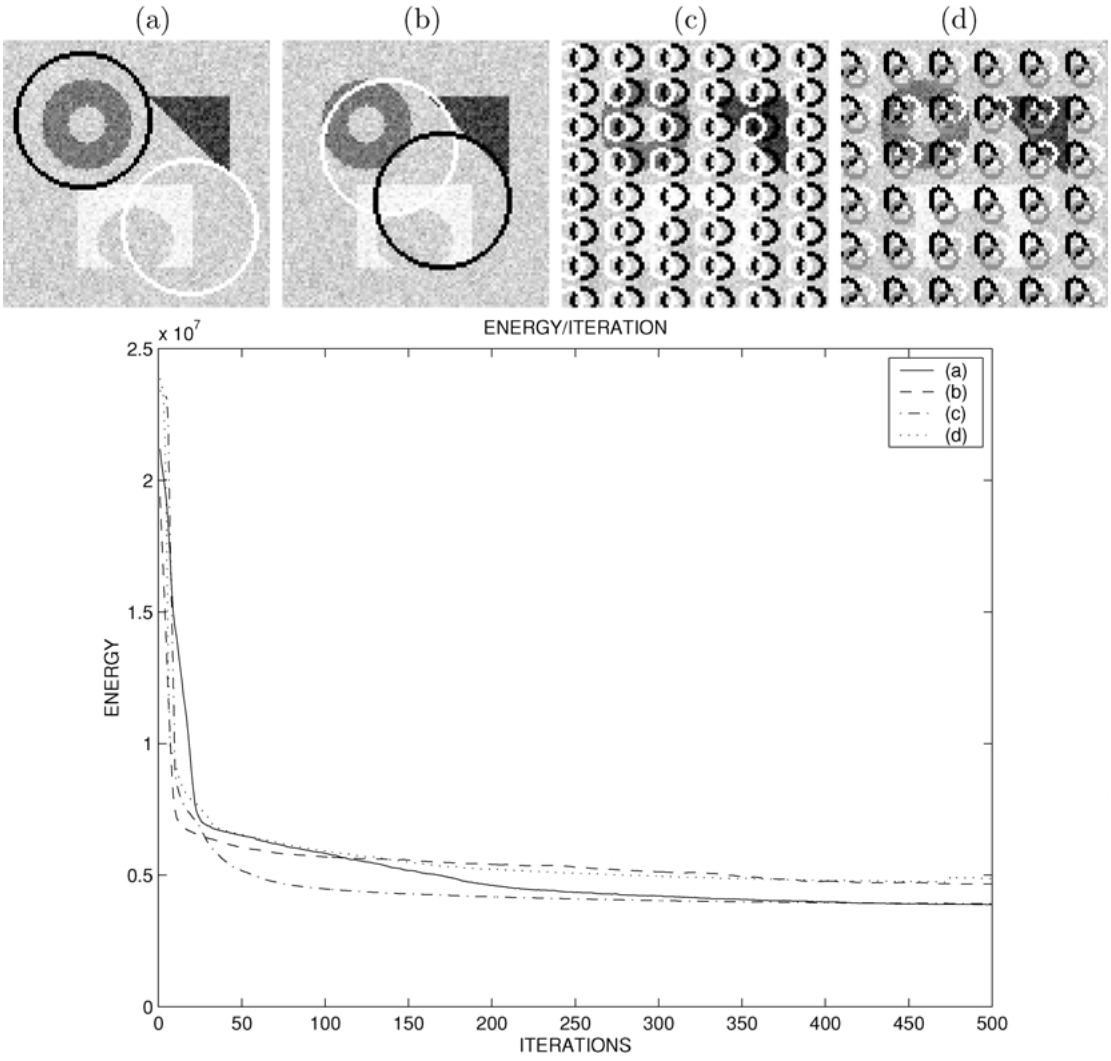

Figure 4. Four different initial conditions and the energies versus iterations.

algorithm is much faster (see Fig. 6 left). In Fig. 6 right, we show a numerical result on the same image with four segments, but using the 8-phase model with 3 level set functions. The correct segmentation is obtained, and four final segments are empty.

In Fig. 7 we show a noisy synthetic image with a triple junction. Using only one level set function, the triple junction cannot be represented. Most of the models need three level set functions, as in Zhao et al. (1996) and Samson et al. (1999, 2000). Here, we need only two level set functions to represent the triple junction. We show their zero level sets, which have to overlap on a segment of the triple junction.

We show next numerical results on two real pictures (an MRI brain image and a house), in Figs. 8, 9 and 10. We use here two level set functions, detecting four phases. We also show the final four segments detected by the algorithm. We see how the model can handle complex topologies, and also that the four phases in Fig. 9 identify quite well the gray matter, the white matter, etc.

In Fig. 11 we show an example of a color RGB image (three channels) with contours without gradient

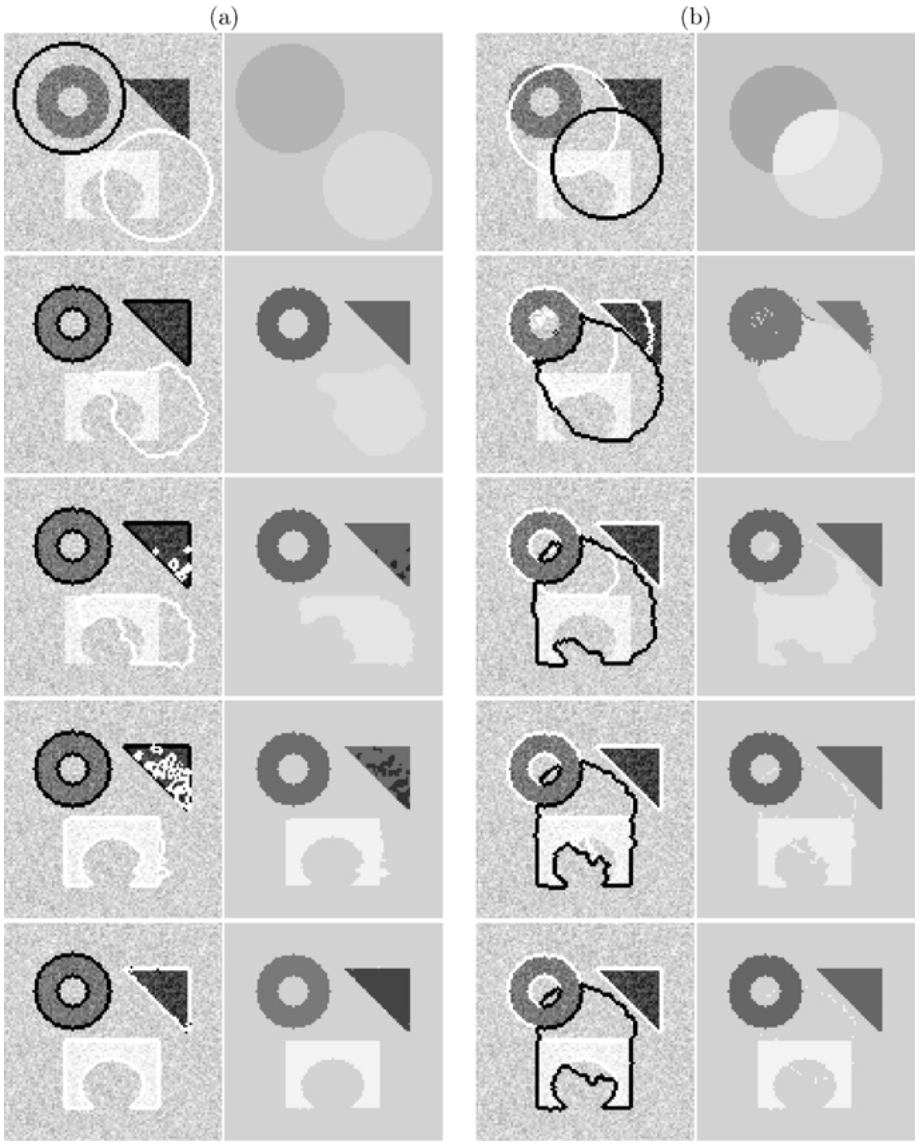

Figure 5. Segmentation of a noisy synthetic image, using the 4-phase piecewise constant model. First and 3rd columns: the evolving contours overlay on the original image; 2nd and 4th columns: computed averages of the four segments $c_{11}, c_{10}, c_{01}, c_{00}$. Left: (a) $\nu = 0.0165 \cdot 255^2$, size $= 100 \times 100$, cpu $= 30.00$ sec. Right: (b) $\nu = 0.0165 \cdot 255^2$, size $= 100 \times 100$, steady state (the algorithm computes only a local minimum in this case).

(cognitive contours following Kanizsa (1997)). We also see that this result is an improvement of the result on the same picture from Chan et al. (2000), where the three objects had the same intensity in the end. Here, the correct intensities are detected, for each object. Again, this generalized model can detect "contours without edges."

In Fig. 12 we show how the model works on another color RGB image, where we use three level set functions ϕ_1, ϕ_2, ϕ_3, representing up to eight phases or colors. The algorithm detects six segments and junctions. In the classical approaches, it would have been necessarily to consider at least six level set functions (here, 2 of the final 8 segments are empty).

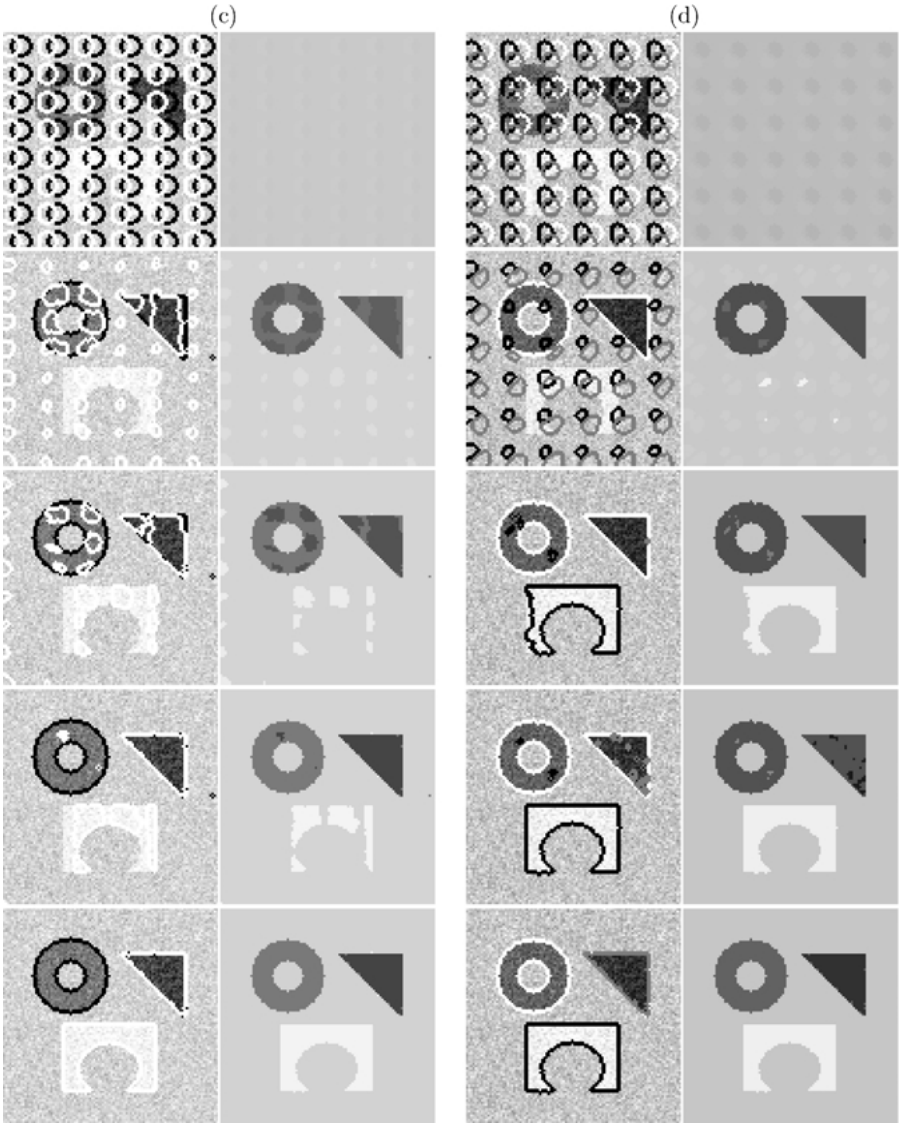

Figure 6. Left: (c) $\nu = 0.0165 \cdot 255^2$, size $= 100 \times 100$, cpu $= 8.46$ sec (very fast). Right: (d) three-level sets evolution with up to 8 phases (at steady state the correct segmentation is obtained, with four segments, while the other four segments are empty). $\nu = 0.0165 \cdot 255^2$, size $= 100 \times 100$.

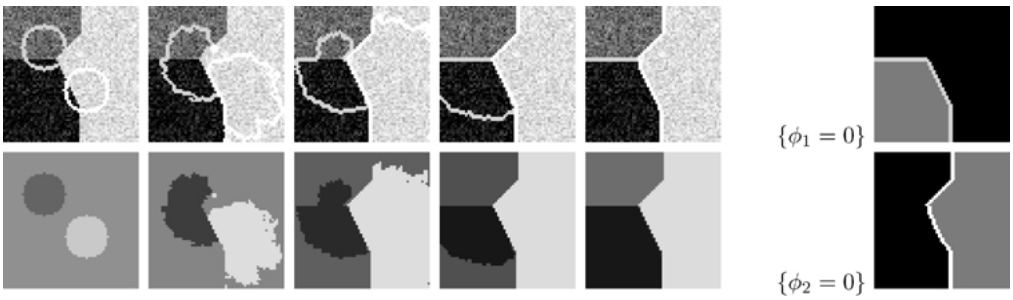

Figure 7. Results on a synthetic image, with a triple junction, using the 4-phase piecewise constant model with 2 level set functions. We also show the zero level sets of ϕ_1 and ϕ_2. $\nu = 0.05 \cdot 255^2$, size $= 64 \times 64$, cpu $= 3.51$ sec.

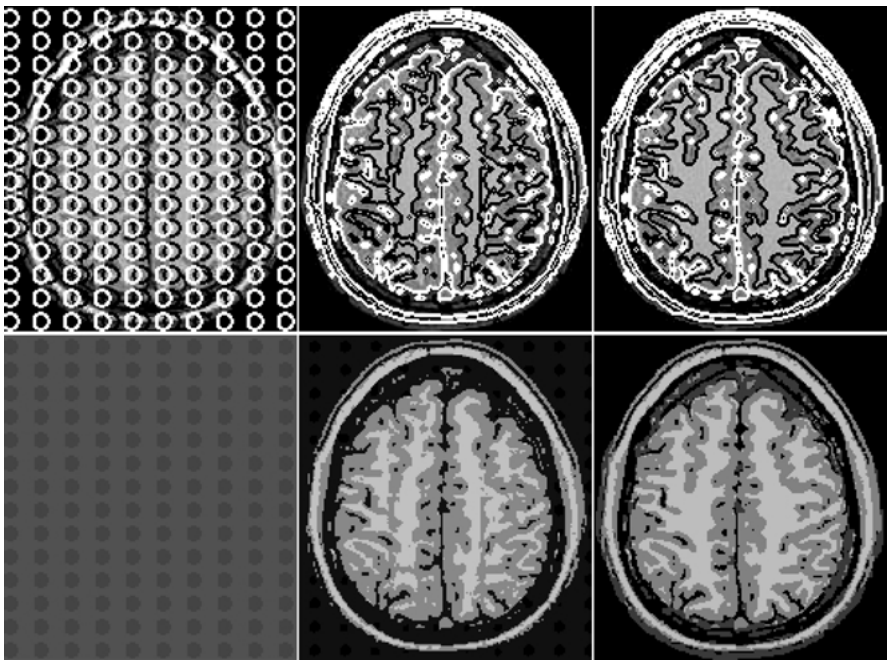

Figure 8. Segmentation of an MRI brain image, using two level set functions and four constant phases. $\nu = 0.01 \cdot 255^2$, size $= 163 \times 181$, cpu $= 12.86$ sec.

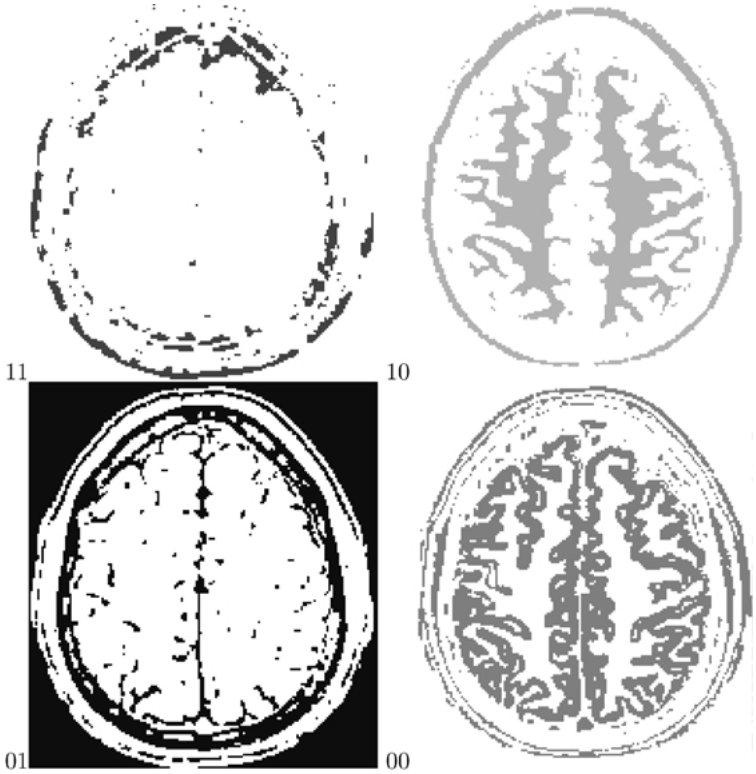

Figure 9. The algorithm depicts quite well the final four segments from the previous result (white matter, gray matter, etc.). The final averages are $c_{11} = 45$, $c_{10} = 159$, $c_{01} = 9$, $c_{00} = 103$.

Figure 10. Segmentation of a real outdoor picture, using two level set functions and four constant phases. In the bottom row, we show the final four segments obtained. The final averages are: $c_{11} = 159$, $c_{10} = 205$, $c_{01} = 23$, and $c_{00} = 97$. $\nu = 0.01 \cdot 255^2$, size $= 103 \times 89$, cpu $= 7.88$ sec.

4.2. Numerical Results in the Piecewise-Smooth Case (1D & 2D)

We begin this part by an experimental result for signal denoising and segmentation. We show in Fig. 13 left an original signal and its noisy version, together with two points, where $\phi = 0$ at the initial time. In Fig. 13 right, we show the segmented signal, and the detected set of jumps given by $\phi = 0$ at the steady state, using the proposed level set algorithm in dimension 1, from Section 3. Note that piecewise-smooth regions are very well reconstructed by the model, and that the jumps are well located and without smearing.

We show in Figs. 14 and 15 two numerical results using the 2-phase algorithm from Section 3: the evolving curves are superposed over the initial noisy image u_0, and the denoised versions u of u_0 are also shown. In Fig. 14, we see that the model performs as active contours, denoising and edge-detection, and several objects of distinct intensities can be correctly segmented with only one level set function. In Fig. 15, we apply the model to a real piecewise-smooth image. As we have already mentioned, similar results with those from Figs. 14 and 15 have been obtained independently and contemporaneously by Tsai et al. (2001).

Finally, we show in Fig. 16 numerical results on a real noisy image, using the four-phase model from Section 3. At the initial time, the two curves given by $\{\phi_1 = 0\}$ and $\{\phi_2 = 0\}$ are shown in different colors (we use again the seed initialization).

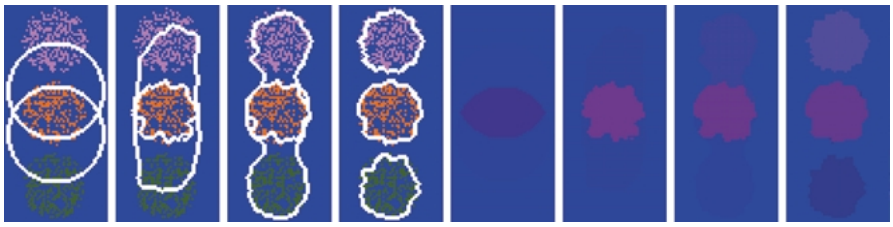

Figure 11. Numerical results on a synthetic color picture. We show in particular that contours not defined by gradient can be detected. These are called cognitive contours (Kanizsa, 1997). $\nu = 0.4 \times 255^2$, size $= 48 \times 100$, cpu $= 42.17$ sec.

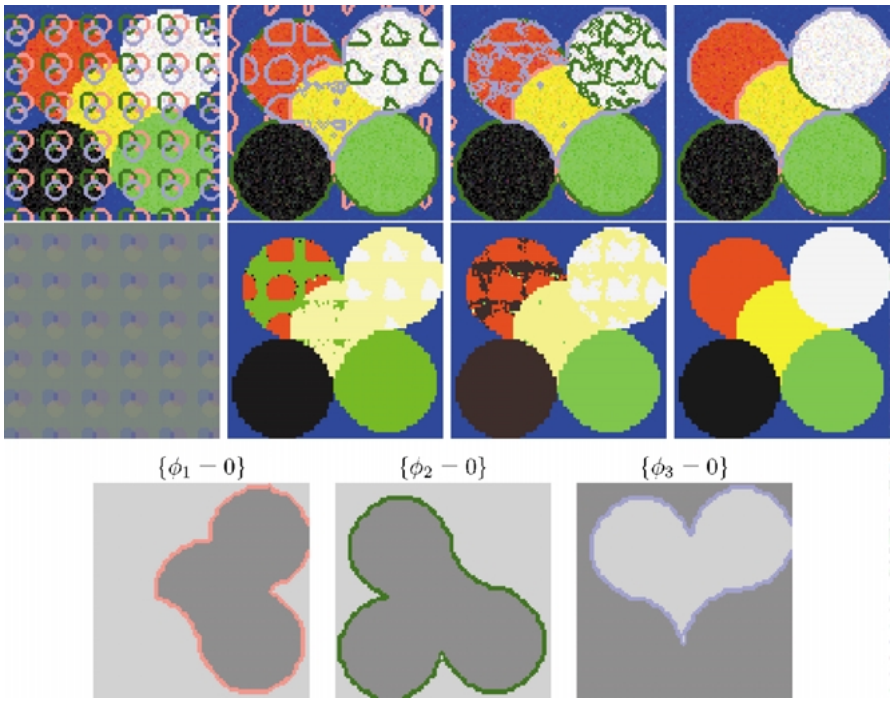

Figure 12. Color noisy picture with junctions. We use three level set functions representing up to eight constant regions. Here six segments are detected. We show the final zero-level sets of ϕ_1, ϕ_2, ϕ_3. $\nu = 0.02 \cdot 255^2$, size $= 100 \times 100$, cpu $= 65.45$ sec.

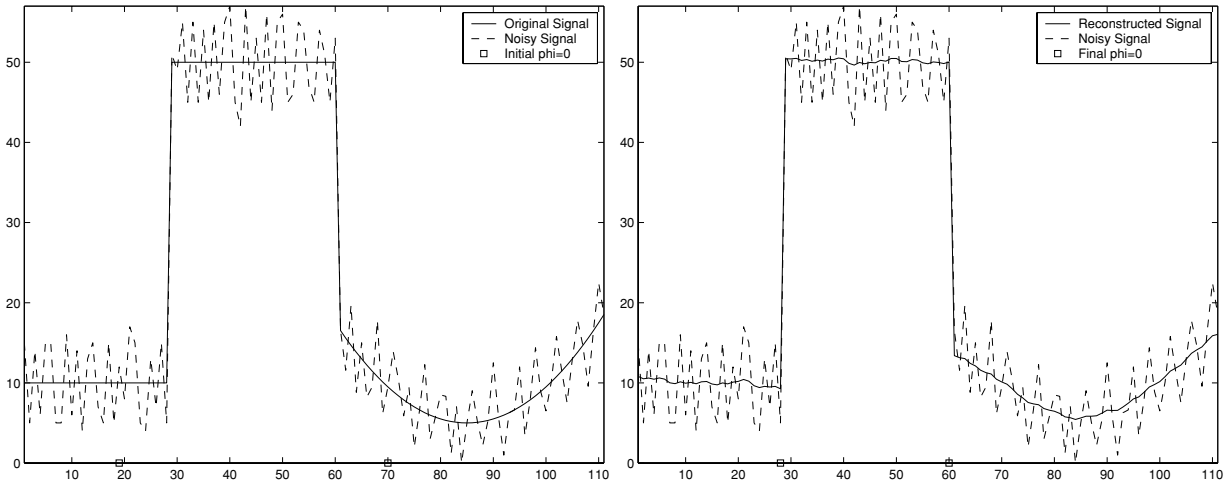

Figure 13. Left: original and noisy signal, together with the set of points where $\phi = 0$ at the initial time, represented by squares on the x-axis. Right: reconstructed signal, noisy signal, and the set of points where $\phi = 0$ at the steady state (the jumps).

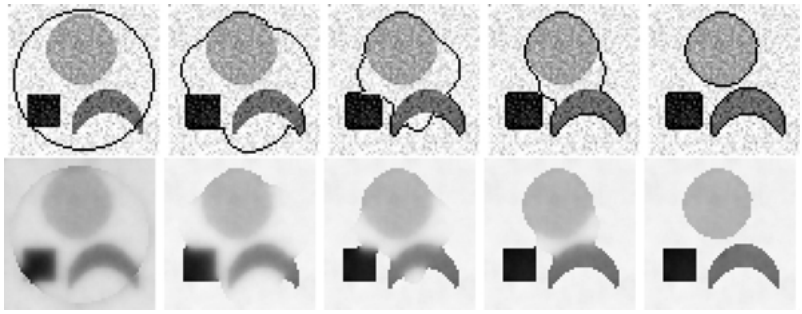

Figure 14. Results on a noisy image, using the 2-phase level set algorithm for the piecewise smooth Mumford-Shah model. The algorithm performs as active contours, denoising and edge detection.

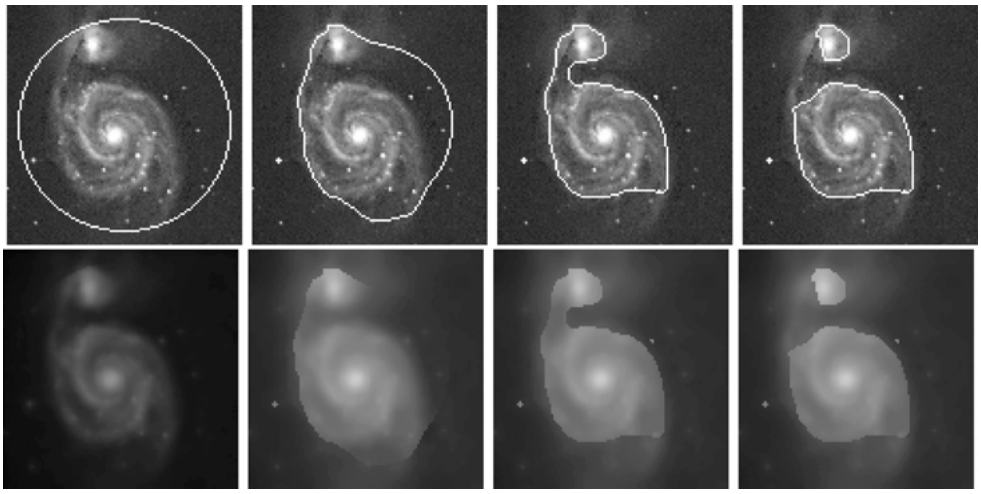

Figure 15. Numerical result using the 2-phase piecewise-smooth Mumford-Shah level set algorithm, on a piecewise-smooth real image. $\nu = 0.0305 * 255^2$, $\mu = 10$, size $= 110 \times 112$.

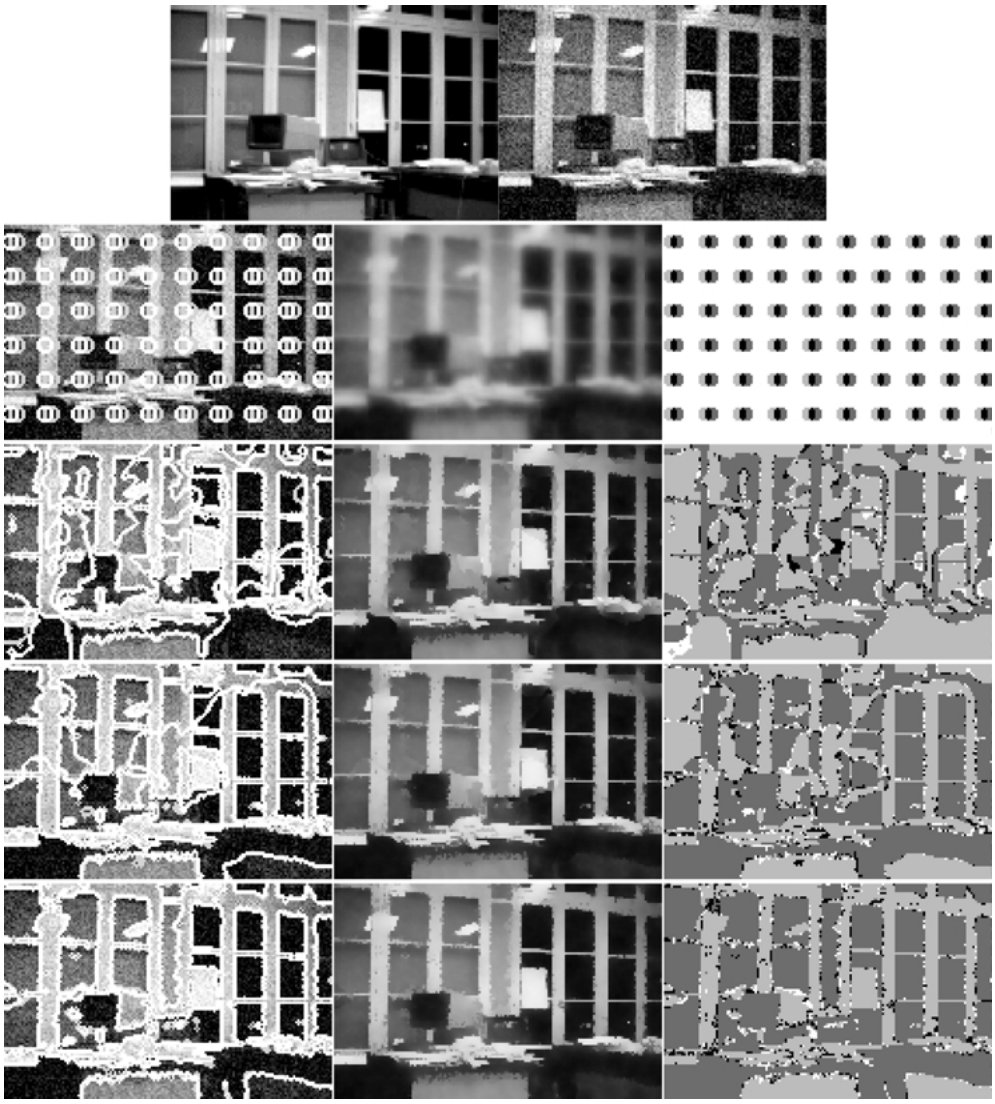

Figure 16. First row: original and noisy image. 2nd–5th rows: curves over u_0, denoised u and the four artificial phases for increasing times, by the 4-phase piecewise-smooth model from Section 3. $\nu = 0.004 * 255^2$, $\mu = 5$, size $= 152 \times 100$, with re-initialization to the distance function.

5. Conclusion

In this paper, we have introduced a new multiphase model for Mumford-Shah image segmentation, by level sets. The proposed model is a common framework to perform active contours, denoising, segmentation, and edge detection. The multiphase formulation is different than the classical approaches, and has the advantages that the phases cannot produce vacuum or overlap, by construction (there is no additional constraint to prevent vacuum or overlap), and it minimizes as much as possible the computational cost, considerably reducing the number of level set functions. We show in particular that triple junctions can be represented and detected using only two level set functions. In the piecewise-constant case, we only need to know an upper bound of the segments, while in the four-phase piecewise-smooth case, we do not need to know a-priori how many segments the image has. These models can be applied to other problems, such as texture segmentation and discrimination. Finally, we validated the proposed models by various numerical results in one and two dimensions.

Appendix: The Description of the Numerical Algorithms

Let $h = \triangle x = \triangle y$ be the space steps, $\triangle t$ be the time step, $\varepsilon = h$, $(x_i, y_j) = (ih, jh)$ be the discrete points, for $1 \le i, j \le M$, and $u_{0,i,j} \approx u_0(x_i, y_j)$, $\phi^n_{i,j} \approx \phi(n\triangle t, x_i, y_j)$, with $n \ge 0$. We set:

$$H_\varepsilon(x) = \frac{1}{2}\left[1 + \frac{2}{\pi}\arctan\left(\frac{x}{\varepsilon}\right)\right],$$
$$\delta_\varepsilon(x) = H'_{2,\varepsilon}(x) = \frac{1}{\pi}\frac{\varepsilon}{\varepsilon^2 + x^2}.$$

A.1. The Piecewise Constant Case

For the purpose of illustration, we give the details of the numerical algorithm for the four-phase model from Section 2, by solving the equations:

$$c_{11}(\Phi) = \frac{\int_\Omega u_0 H_\varepsilon(\phi_1) H_\varepsilon(\phi_2)\,dx\,dy}{\int_\Omega H_\varepsilon(\phi_1) H_\varepsilon(\phi_2)\,dx\,dy},$$

$$c_{10}(\Phi) = \frac{\int_\Omega u_0 H_\varepsilon(\phi_1)(1 - H_\varepsilon(\phi_2))\,dx\,dy}{\int_\Omega H_\varepsilon(\phi_1)(1 - H_\varepsilon(\phi_2))\,dx\,dy},$$

$$c_{01}(\Phi) = \frac{\int_\Omega u_0 (1 - H_\varepsilon(\phi_1)) H_\varepsilon(\phi_2)\,dx\,dy}{\int_\Omega (1 - H_\varepsilon(\phi_1)) H_\varepsilon(\phi_2)\,dx\,dy},$$

$$c_{00}(\Phi) = \frac{\int_\Omega u_0 (1 - H_\varepsilon(\phi_1)) H_\varepsilon(\phi_2)\,dx\,dy}{\int_\Omega (1 - H_\varepsilon(\phi_1)) H_\varepsilon(\phi_2)\,dx\,dy},$$

$$\begin{aligned}\frac{\partial \phi_1}{\partial t} &= \delta_\varepsilon(\phi_1)\left\{\nu \operatorname{div}\left(\frac{\nabla \phi_1}{|\nabla \phi_1|}\right)\right.\\ &\quad - [((u_0 - c_{11})^2 - (u_0 - c_{01})^2) H(\phi_2)\\ &\quad \left. + ((u_0 - c_{10})^2 - (u_0 - c_{00})^2)(1 - H(\phi_2))]\right\},\\ \frac{\partial \phi_2}{\partial t} &= \delta_\varepsilon(\phi_2)\left\{\nu \operatorname{div}\left(\frac{\nabla \phi_2}{|\nabla \phi_2|}\right)\right.\\ &\quad - [((u_0 - c_{11})^2 - (u_0 - c_{10})^2) H(\phi_1)\\ &\quad \left. + ((u_0 - c_{01})^2 - (u_0 - c_{00})^2)(1 - H(\phi_1))]\right\}.\end{aligned}$$

Set $n = 0$, $\phi^0_{1,i,j}$ and $\phi^0_{2,i,j}$ given (the initial set of curves). For each $n > 0$ until steady state:

1. compute by the above formulas the averages c^n_{11}, c^n_{10}, c^n_{01}, c^n_{00}.
2. compute $\phi^{n+1}_{1,i,j}$, $\phi^{n+1}_{2,i,j}$ as follows (using a semi-implicit finite differences scheme): let

$$C_1 = \frac{1}{\sqrt{\left(\frac{\phi^n_{1,i+1,j} - \phi^n_{1,i,j}}{h}\right)^2 + \left(\frac{\phi^n_{1,i,j+1} - \phi^n_{1,i,j-1}}{2h}\right)^2}},$$
$$C_2 = \frac{1}{\sqrt{\left(\frac{\phi^n_{1,i,j} - \phi^n_{1,i-1,j}}{h}\right)^2 + \left(\frac{\phi^n_{1,i-1,j+1} - \phi^n_{1,i-1,j-1}}{2h}\right)^2}},$$
$$C_3 = \frac{1}{\sqrt{\left(\frac{\phi^n_{1,i+1,j} - \phi^n_{1,i-1,j}}{2h}\right)^2 + \left(\frac{\phi^n_{1,i,j+1} - \phi^n_{1,i,j}}{h}\right)^2}},$$
$$C_4 = \frac{1}{\sqrt{\left(\frac{\phi^n_{1,i+1,j-1} - \phi^n_{1,i-1,j-1}}{2h}\right)^2 + \left(\frac{\phi^n_{1,i,j} - \phi^n_{1,i,j-1}}{h}\right)^2}}.$$

Let $m_1 = \frac{\triangle t}{h^2}\delta_\varepsilon(\phi_{1,i,j})\nu$, $C = 1 + m_1(C_1 + C_2 + C_3 + C_4)$,

$$\begin{aligned}\phi^{n+1}_{1,i,j} = \frac{1}{C}\big[&\phi^n_{1,i,j} + m_1\big(C_1\phi^n_{1,i+1,j} + C_2\phi^n_{1,i-1,j}\\ &+ C_3\phi^n_{1,i,j+1} + C_4\phi^n_{1,i,j-1}\big)\\ &+ \triangle t\,\delta_\varepsilon(\phi_{1,i,j})\big(-\big(u_{0,i,j} - c^n_{11}\big)^2 H_\varepsilon\big(\phi^n_{2,i,j}\big)\\ &- \big(u_{0,i,j} - c^n_{10}\big)^2\big(1 - H_\varepsilon\big(\phi^n_{2,i,j}\big)\big)\\ &+ \big(u_{0,i,j} - c^n_{01}\big)^2 H_\varepsilon\big(\phi^n_{2,i,j}\big)\\ &+ \big(u_{0,i,j} - c^n_{00}\big)^2\big(1 - H_\varepsilon\big(\phi^n_{2,i,j}\big)\big)\big)\big].\end{aligned}$$

Similarly, let

$$D_1 = \frac{1}{\sqrt{\left(\frac{\phi^n_{2,i+1,j} - \phi^n_{2,i,j}}{h}\right)^2 + \left(\frac{\phi^n_{2,i,j+1} - \phi^n_{2,i,j-1}}{2h}\right)^2}},$$
$$D_2 = \frac{1}{\sqrt{\left(\frac{\phi^n_{2,i,j} - \phi^n_{2,i-1,j}}{h}\right)^2 + \left(\frac{\phi^n_{2,i-1,j+1} - \phi^n_{2,i-1,j-1}}{2h}\right)^2}},$$
$$D_3 = \frac{1}{\sqrt{\left(\frac{\phi^n_{2,i+1,j} - \phi^n_{2,i-1,j}}{2h}\right)^2 + \left(\frac{\phi^n_{2,i,j+1} - \phi^n_{2,i,j}}{h}\right)^2}},$$
$$D_4 = \frac{1}{\sqrt{\left(\frac{\phi^n_{2,i+1,j-1} - \phi^n_{2,i-1,j-1}}{2h}\right)^2 + \left(\frac{\phi^n_{2,i,j} - \phi^n_{2,i,j-1}}{h}\right)^2}}.$$

Let $m_2 = \frac{\triangle t}{h^2}\delta_\varepsilon(\phi_{2,i,j})\nu$, $D = 1 + m_2(D_1 + D_2 + D_3 + D_4)$,

$$\begin{aligned}\phi_{2,i,j}^{n+1} = \frac{1}{D}\big[&\phi_{2,i,j}^n + m_2\big(D_1\phi_{2,i+1,j}^n + D_2\phi_{2,i-1,j}^n \\ &+ D_3\phi_{2,i,j+1}^n + D_4\phi_{2,i,j-1}^n\big) \\ &+ \triangle t\delta_\varepsilon\big(\phi_{2,i,j}\big)\big(-\big(u_{0,i,j} - c_{11}^n\big)^2 H_\varepsilon\big(\phi_{1,i,j}^n\big) \\ &+ \big(u_{0,i,j} - c_{10}^n\big)^2 H_\varepsilon\big(\phi_{1,i,j}^n\big) \\ &- \big(u_{0,i,j} - c_{01}^n\big)^2\big(1 - H_\varepsilon\big(\phi_{1,i,j}^n\big)\big) \\ &+ \big(u_{0,i,j} - c_{00}^n\big)^2\big(1 - H_\varepsilon\big(\phi_{1,i,j}^n\big)\big)\big)\big].\end{aligned}$$

A.2. The Piecewise Smooth Case

We give here the details of the numerical algorithm for solving the following equations from Section 3, written in the form:

$$\begin{aligned}u^+ H_\varepsilon(\phi) &= u_0 H_\varepsilon(\phi) + \mu\,\mathrm{div}(H_\varepsilon(\phi)\nabla u^+), \\ u^-(1-H_\varepsilon(\phi)) &= u_0(1-H_\varepsilon(\phi)) \\ &\quad + \mu\,\mathrm{div}((1 - H_\varepsilon(\phi))\nabla u^-), \\ \frac{\partial\phi}{\partial t} &= \delta_\varepsilon(\phi)\bigg[\nu\nabla\bigg(\frac{\nabla\phi}{|\nabla\phi|}\bigg) - |u^+ - u_0|^2 \\ &\quad - \mu|\nabla u^+|^2 + |u^- - u_0|^2 + \mu|\nabla u^-|^2\bigg].\end{aligned}$$

Set $n = 0$, $\phi_{i,j}^0$ given (the initial curve). For each $n > 0$ until steady state:

(1) compute $u_{i,j}^{n,+}$ and $u_{i,j}^{n,-}$,
(2) compute a C^1 extension of $u_{i,j}^{n,+}$ to $\{\phi_{i,j}^n \le 0\}$ and a C^1 extension of $u_{i,j}^{n,-}$ to $\{\phi_{i,j}^n \ge 0\}$,
(3) compute $\phi_{i,j}^{n+1}$, as follows:

$$\begin{aligned}c &= H_\varepsilon\big(\phi_{i,j}^n\big) + \frac{\mu}{h^2}\big(2H_\varepsilon\big(\phi_{i,j}^n\big) + H_\varepsilon\big(\phi_{i-1,j}^n\big) \\ &\quad + H_\varepsilon\big(\phi_{i,j-1}^n\big)\big), \\ u_{i,j}^{n+1,+} &= \frac{1}{c}\bigg[\frac{\mu}{h^2}\big(H_\varepsilon\big(\phi_{i,j}^n\big)u_{i+1,j}^{n,+} + H_\varepsilon\big(\phi_{i-1,j}^n\big)u_{i-1,j}^{n,+} \\ &\quad + H_\varepsilon\big(\phi_{i,j}^n\big)u_{i,j+1}^{n,+} + H_\varepsilon\big(\phi_{i,j-1}^n\big)u_{i,j-1}^{n,+}\big) \\ &\quad + H_\varepsilon\big(\phi_{i,j}^n\big)u_{0,i,j}\bigg],\end{aligned}$$

$$\begin{aligned}d &= \big(1 - H_\varepsilon\big(\phi_{i,j}^n\big)\big) + \frac{\mu}{h^2}\big(2\big(1 - H_\varepsilon\big(\phi_{i,j}^n\big)\big) \\ &\quad + \big(1 - H_\varepsilon\big(\phi_{i-1,j}^n\big)\big) + \big(1 - H_\varepsilon\big(\phi_{i,j-1}^n\big)\big)\big),\end{aligned}$$

$$\begin{aligned}u_{i,j}^{n+1,-} = \frac{1}{d}\bigg[&\frac{\mu}{h^2}\big(\big(1 - H_\varepsilon\big(\phi_{i,j}^n\big)\big)u_{i+1,j}^{n,-} \\ &+ \big(1 - H_\varepsilon\big(\phi_{i-1,j}^n\big)\big)u_{i-1,j}^{n,-} \\ &+ \big(1 - H_\varepsilon\big(\phi_{i,j}^n\big)\big)u_{i,j+1}^{n,-} \\ &+ \big(1 - H_\varepsilon\big(\phi_{i,j-1}^n\big)\big)u_{i,j-1}^{n,-} \\ &+ \big(1 - H_\varepsilon\big(\phi_{i,j}^n\big)\big)u_{0,i,j}\bigg],\end{aligned}$$

$$C_1 = \frac{1}{\sqrt{\left(\frac{\phi_{i+1,j}^n - \phi_{i,j}^n}{h}\right)^2 + \left(\frac{\phi_{i,j+1}^n - \phi_{i,j-1}^n}{2h}\right)^2}},$$

$$C_2 = \frac{1}{\sqrt{\left(\frac{\phi_{i,j}^n - \phi_{i-1,j}^n}{h}\right)^2 + \left(\frac{\phi_{i-1,j+1}^n - \phi_{i-1,j-1}^n}{2h}\right)^2}},$$

$$C_3 = \frac{1}{\sqrt{\left(\frac{\phi_{i+1,j}^n - \phi_{i-1,j}^n}{2h}\right)^2 + \left(\frac{\phi_{i,j+1}^n - \phi_{i,j}^n}{h}\right)^2}},$$

$$C_4 = \frac{1}{\sqrt{\left(\frac{\phi_{i+1,j-1}^n - \phi_{i-1,j-1}^n}{2h}\right)^2 + \left(\frac{\phi_{i,j}^n - \phi_{i,j-1}^n}{h}\right)^2}}.$$

Let $m = \frac{\triangle t}{h^2}\delta_\varepsilon(\phi_{i,j})\nu$, $C = 1 + m(C_1 + C_2 + C_3 + C_4)$.

$$\mathrm{grad}_{i,j}^{n,+} = \left(\frac{u_{i+1,j}^{n,+} - u_{i-1,j}^{n,+}}{2h}\right)^2 + \left(\frac{u_{i,j+1}^{n,+} - u_{i,j-1}^{n,+}}{2h}\right)^2,$$

$$\mathrm{grad}_{i,j}^{n,-} = \left(\frac{u_{i+1,j}^{n,-} - u_{i-1,j}^{n,-}}{2h}\right)^2 + \left(\frac{u_{i,j+1}^{n,-} - u_{i,j-1}^{n,-}}{2h}\right)^2,$$

$$\begin{aligned}\phi_{i,j}^{n+1} = \frac{1}{C}\big[&\phi_{i,j}^n + m\big(C_1\phi_{i+1,j}^n + C_2\phi_{i-1,j}^n \\ &+ C_3\phi_{i,j+1}^n + C_4\phi_{i,j-1}^n\big) + \triangle t\delta_\varepsilon(\phi_{i,j}) \\ &\times \big(-\big(u_{0,i,j} - u_{i,j}^{n,+}\big)^2 + \big(u_{0,i,j} - u_{i,j}^{n,-}\big)^2 \\ &- \mu\,\mathrm{grad}_{i,j}^{n,+} + \mu\,\mathrm{grad}_{i,j}^{n,-}\big)\big].\end{aligned}$$

We need the extension from step 2) above, to compute the jumps $(u^+ - u_0)^2 - (u^- - u_0)^2$, $|\nabla u^+|^2 - |\nabla u^-|^2$ along the curve. For instance, to extend u^+ to the region $\{\phi \le 0\}$, we solve $\triangle u^+ = 0$ on $\{\phi \le 0\}$, with given prescribed values on $\{\phi > 0\}$. This can be done by iterating the scheme: $u_{i,j}^{k+1,+} = 0.25(u_{i+1,j}^{k,+} + u_{i,j+1}^{k,+} + u_{i-1,j}^{k,+} + u_{i,j-1}^{k,+})$, where $u^{0,+} = u^{n,+}$ (n is fixed for varying k). Other possibilities for the extension step

can be found in Zhao et al. (1996), Chen et al. (1997), Fedkiw et al. (1999), Fedkiw (1999), Jensen (1993), and Caselles et al. (1997).

A usual procedure, when working with level set functions, is reinitialization to the distance function. We have used this procedure only in the last numerical result from Fig. 16. For details, we refer to Sussman et al. (1994).

Acknowledgments

The first author thanks to P. Burchard and R. March for their useful remarks and suggestions, and also to G.P. Leonardi, for pointing out to us interesting references on minimal partition problems. Both authors thank the unknown referees from IJCV and VLSM, for their very interesting remarks and suggestions, which helped enormously to improve the presentation of this paper, and also the organizing committee of VLSM, the Guest Editors O. Faugeras and N. Paragios. This work has been supported in part by grants NSF/DMS-9973341, NSF/ITR-0113439, ONR N00014-96-1-0277, and NIH P20MH65166.

References

Amadieu, O., Debreuve, E., Barlaud, M., and Aubert, G. 1999. Inward and outward curve evolution using level set method. In *Proceedings ICIP*, Japan, pp. 188–192.

Ambrosio, L. 1989. A compactness theorem for a special class of functions of bounded variation. *Boll. Un. Mat. It*., 3(B):857–881.

Ambrosio, L. and Tortorelli, V.M. 1990. Approximation of functionals depending on jumps by elliptic functionals via $\Gamma-$convergence. *Comm. Pure Appl. Math*., 43:999–1036.

Ambrosio, L. and Tortorelli, V.M. 1992. On the approximation of free discontinuity problems. *Bolletino U.M.I*., 7(6-B):105–123.

Aubert, G. and Kornprobst, P. 2001. *Mathematical Problems in Image Processing. Partial Differential Equations and the Calculus of Variations*. Applied Mathematical Sciences, vol. 147, Springer: New York.

Barles, G. 1994. Solutions de viscosité des équations de Hamilton-Jacobi. *Mathématiques & Applications*, vol. 17, Springer-Verlag.

Barles, G. and Souganidis, P.E. 1998. A new approach to front propagation problems: theory and applications. *Arch. Rational Mech. Analysis*, 141(3):237–296.

Bourdin, B. 1999. Image segmentation with a finite element method. *M2AN Math. Model. Numer. Anal*., 33(2):229–244.

Bourdin, B. and Chambolle, A. 2000. Implementation of a finite-elements approximation of the Mumford-Shah functional. *Numer. Math*., 85(4):609–646.

Caselles, V., Morel, J.M., and Sbert, C. 1998. An axiomatic approach to image interpolation. *IEEE-IP*, 7(3):376–386.

Chambolle, A. 1992. Un théorème de Γ-convergence pour la segmentation des signaux. *C. R. Acad. Sci. Paris*, 314(I):191–196.

Chambolle, A. 1995. Image segmentation by variational methods: Mumford and Shah functional and the discrete approximations. *SIAM J. Appl. Math*., 55(3):827–863.

Chambolle, A. 1999. Finite-differences discretizations of the Mumford-Shah functional. *M2AN Math. Model. Numer. Anal*., 33(2):261–288.

Chambolle, A. and Dal Maso, G. 1999. Discrete approximation of the Mumford-Shah functional in dimension two. *M2AN Math. Model. Numer. Anal*., 33(4):651–672.

Chan, T. and Vese, L. 1999. An active contour model without edges. In *Scale-Space'99*, M. Nilsen et al. (Eds.), LNCS, vol. 1682, pp. 141–151.

Chan, T. and Vese, L. 2001. Active contours without edges. *IEEE-IP*, 10(2):266–277.

Chan, T., Sandberg, B.Y., and Vese, L. 2000. Active contours without edges for vector-valued images. *JVCIR*, 11:130–141.

Chen, Y.G., Giga, Y., and Goto, S. 1991. Uniqueness and existence of viscosity solutions of generalized mean curvature flow equations. *J. Diff. Geometry*, 33:749–786.

Chen, S., Merriman, B., Osher, S., and Smereka, P. 1997. A simple level set method for solving Stefan problems. *JCP*, 135:8–29.

Cohen, L.D. 1997. Avoiding local minima for deformable curves in image analysis. In *Curves and Surfaces with Applications in CAGD*, A. Le Méhauté, C. Rabut, and L.L. Schumaker (Eds.), pp. 77–84.

Cohen, L., Bardinet, E., and Ayache, N. 1993. Surface reconstruction using active contour models. In *Proceedings SPIE 93 Conference on Geometric Methods in Computer Vision*, San Diego, CA, July 1993.

Crandall, M.G., Ishii, H., and Lions, P.-L. 1992. User's guide to viscosity solutions of second order partial differential equations. *Amer. Math. Soc. Bull*., 27:1–67.

Dal Maso, G., Morel, J.M., and Solimini, S. 1992. A variational method in image segmentation: existence and approximation results. *Acta Matematica*, 168:89–151.

De Giorgi, E. and Ambrosio, L. 1988. New functionals in the calculus of variations. *Atti. Accad. Naz. Lincei Rend. Cl. Sci. Fis. Mat. Natur*., 82(2):199–210.

De Giorgi, E., Carriero, M., and Leaci, A. 1989. Existence theorem for a minimum problem with free discontinuity set. *Arch. Rational Mech. Anal*., 108(3):195–218.

Ei, S.-I., Ikota, R., and Mimura, M. 1999. Segregating partition problem in competition-diffusion systems. *Interfaces and Free Boundaries*, 1(1):57–80.

Evans, L.C. and Gariepy, R.F. 1992. *Measure Theory and Fine Properties of Functions*. CRC Press: Boca Raton, FL.

Evans, L.C. and Spruck, J. 1991. Motion of level sets by mean curvature. *J. Diff. Geometry*, 33:635–681.

Fedkiw, R.P. 1999. The ghost fluid method for discontinuities and interfaces. In *Proceedings of Godunov Methods: Theory and Applications*, Oxford, UK, October 1999.

Fedkiw, R.P., Aslam, T., Merriman, B., and Osher, S. 1999. A non-oscillatory eulerian approach to interfaces in multimaterial flows (the ghost fluid method). *JCP*, 152:457–492.

Guichard, F. and Morel, J.-M. Image Analysis and P.D.E.'s (to appear).

Jensen, R. 1993. Uniqueness of Lipschitz extensions: Minimizing the sup norm of the gradient. *Arch. Rat. Mech. Anal*., 123:51–74.

Kanizsa, G. 1997. La grammaire du voir. Essais sur la perception. Diderot Editeur, Arts et Sciences.

Koepfler, G., Lopez, C., and Morel, J.M. 1994. A multiscale algorithm for image segmentation by variational method. *SIAM J. of Numerical Analysis*, 31(1):282–299.

Leonardi, G.P. and Tamanini, I. 1998. On minimizing partitions with infinitely many components. *Ann. Univ. Ferrara-Sez. VII-Sc. Mat.*, XLIV:41-57.

Lorigo, L.M., Faugeras, O., Grimson, W.E.L., Keriven, R., and Kikinis, R. 1999. Co-dimension 2 geodesic active contours for MRA segmentation. *Information Processing in Medical Imaging, Proceedings*, LNCS, vol. 1613, pp. 126–139.

March, R. 1992. Visual Reconstruction with discontinuities using variational methods. *IVC*, 10:30–38.

Massari, U. and Tamanini, I. 1993. On the finiteness of optimal partitions. *Ann. Univ. Ferrara-Sez. VII-Sc. Mat.*, XXXIX: 167–185.

Merriman, B., Bence, J.K., and Osher, S. 1994. Motion of multiple junctions: A level set approach. *JCP*, 112(2):334–363.

Morel, J.M. and Solimini, S. 1988. Segmentation of images by variational methods: A constructive approach. *Revista Matematica Universidad Complutense de Madrid*, 1:169–182.

Morel, J.M. and Solimini, S. 1989. Segmentation d'images par méthode variationnelle: Une preuve constructive d'existence. *CRASS Paris Série I, Math.*, 308:465–470.

Morel, J.M. and Solimini, S. 1994. *Variational Methods in Image Segmentation*. PNLDE, vol. 14, Birkhäuser: Basel.

Mumford, D., Nitzberg, M., and Shiota, T. 1993. *Filtering, Segmentation and Depth*. LNCS, vol. 662, Springer-Verlag: Berlin.

Mumford, D. and Shah, J. 1989. Optimal approximation by piecewise smooth functions and associated variational problems. *Comm. Pure Appl. Math.* 42:577–685.

Osher, S. and Fedkiw, R.P. 2001. Level set methods: An overview and some recent results. *JCP*, 169(2):463–502.

Osher, S.J. and Fedkiw, R. 2002. *Level Set Methods and Dynamic Implicit Surfaces*. Applied Mathematical Science, vol. 153, Springer.

Osher, S. and Sethian, J.A. 1988. Fronts propagating with curvature-dependent speed: Algorithms based on Hamilton-Jacobi formulation. *JCP*, 79:12–49.

Paragios, N. and Deriche, R. 2000. Coupled Geodesic active regions for image segmentation: A level set approach. In *Proceedings ECCV*, Dublin, vol. II, pp. 224–240.

Samson, C., Blanc-Féraud, L., Aubert, G., and Zerubia, J. 1999. A level set model for image classification. In *Scale-Space'99*, M. Nilsen et al. (Eds.), LNCS, vol. 1682, Springer-Verlag: Berlin, pp. 306–317.

Samson, C., Blanc-Féraud, L., Aubert, G., and Zerubia, J. 2000. A level set model for image classification. *IJCV*, 40(3):187–197.

Sapiro, G. 2001. *Geometric Partial Differential Equations and Image Analysis*. Cambridge University Press: Cambridge, UK.

Sethian, J.A. 1999. *Fast Marching Methods and Level Set Methods: Evolving Interfaces in Computational Geometry, Fluid Mechanics, Computer Vision and Materials Sciences*. Cambridge University Press: Cambridge, UK.

Shah, J. 1996. A common framework for curve evolution, segmentation and anisotropic diffusion. In *Proceedings CVPR*, pp. 136–142.

Shah, J. 1999. Riemannian Drums, Anisotropic Curve Evolution and Segmentation. In *Scale-Space'99*, M. Nilsen et al. (Eds.), LNCS, vol. 1682, Springer-Verlag: Berlin, pp. 129–140.

Sharon, E., Brandt, A., and Basri, R. 2000. Fast multiscale image segmentation. In *Proceedings CVPR*, South Carolina, pp. 70–77.

Shi, J. and Malik, J. 2000. Normalized cuts and image segmentation. *IEEE-PAMI*, 22(8):888–905.

Smith, K.A., Solis, F.J., and Chopp, D. 2002. A projection method for motion of triple junctions by level sets. *Interfaces and Free Boundaries*, 4(3):263–276.

Sussman, M., Smereka, P., and Osher, S. 1994. A level set approach for computing solutions to incompressible two-phase flows. *JCP*, 119:146–159.

Tamanini, I. 1996. Optimal approximation by piecewise constant functions. *Progress in Nonlinear Differential Equations and Their Applications*, Birkhäuser Verlag, 25:73–85.

Tamanini, I. and Congedo, G. 1996. Optimal segmentation of unbounded functions. *Rend. Sem. Mat. Univ. Padova*, 95:153–174.

Tsai, A., Yezzi, A., and Willsky, A.S. 2001. Curve evolution implementation of the Mumford-Shah functional for image segmentation, denoising, interpolation, and magnification. *IEEE-IP*, 10(8): 1169–1186.

Yezzi, A., Tsai, A., and Willsky, A. 1999. A statistical approach to snakes for bimodal and trimodal imagery. In *Proceedings ICCV*, pp. 898–903.

Zhao, H.-K., Chan, T., Merriman, B. and Osher, S. 1996. A variational level set approach to multiphase motion. *JCP* 127:179–195.

Zhu, S.C., Lee, T.S., and Yuille, A.L. 1995. Region competition: Unifying snakes, region growing, Energy/Bayes/MDL for multi-band image segmentation. In *Proceedings ICCV*, Cambridge, pp. 416–423.

Zhu, S.C. and Yuille, A. 1996. Region competition: Unifying snakes, region growing, and Bayes/MDL for multi-band image segmentation. *IEEE-PAMI*, 18:884–900.